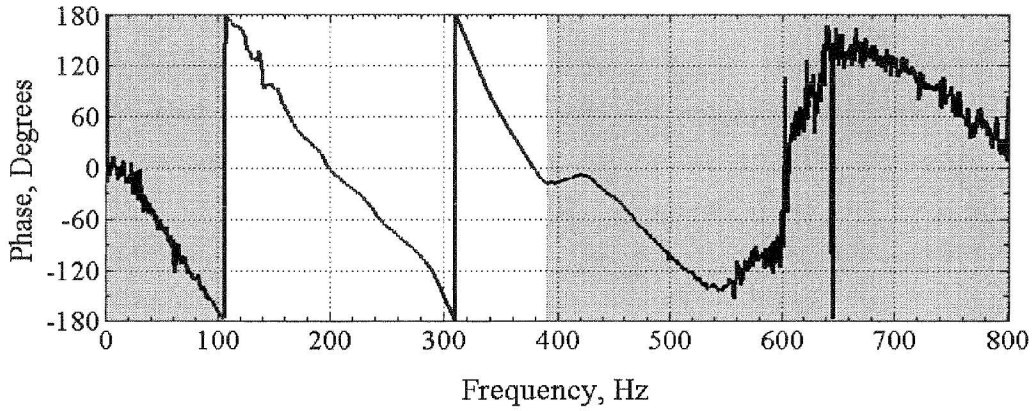

Figure X.4 Phase Plots Measured by SASW Testing with 2-ft Receiver Spacing (4E6_F_43.DAT)

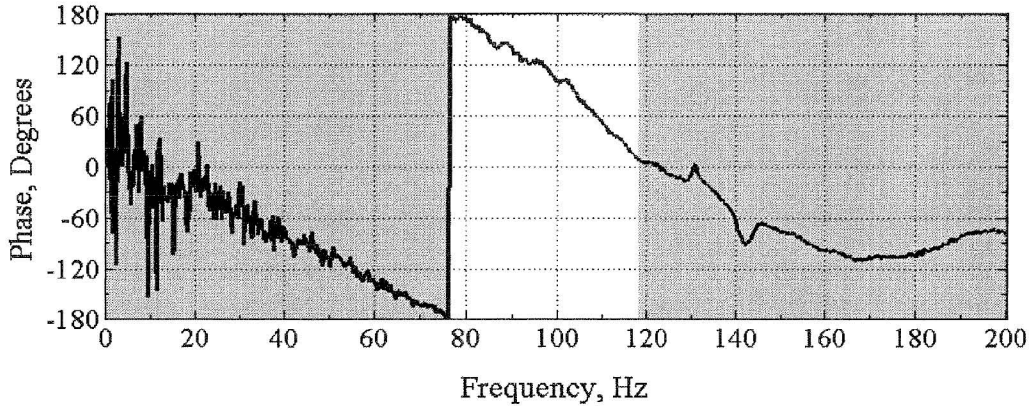

Figure X.5 Phase Plots Measured by SASW Testing with 3-ft Receiver Spacing (4E3_F_21.DAT)

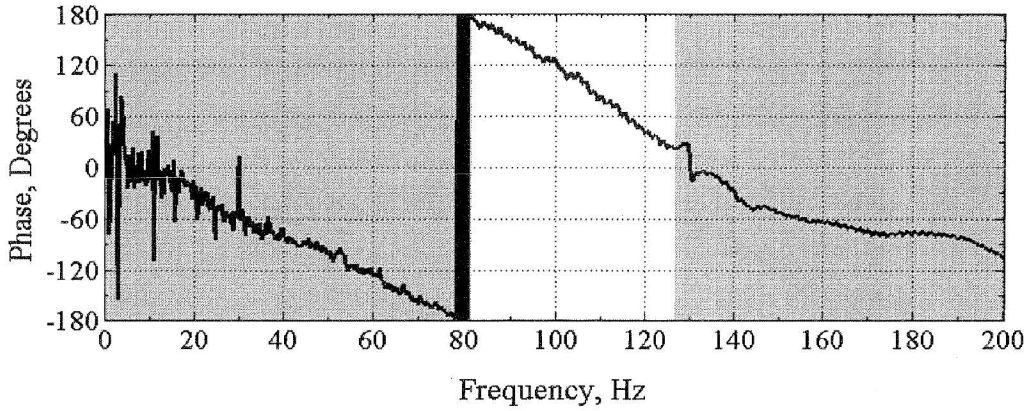

Figure X.6 Phase Plots Measured by SASW Testing with 3-ft Receiver Spacing (4E4_F_21.DAT)

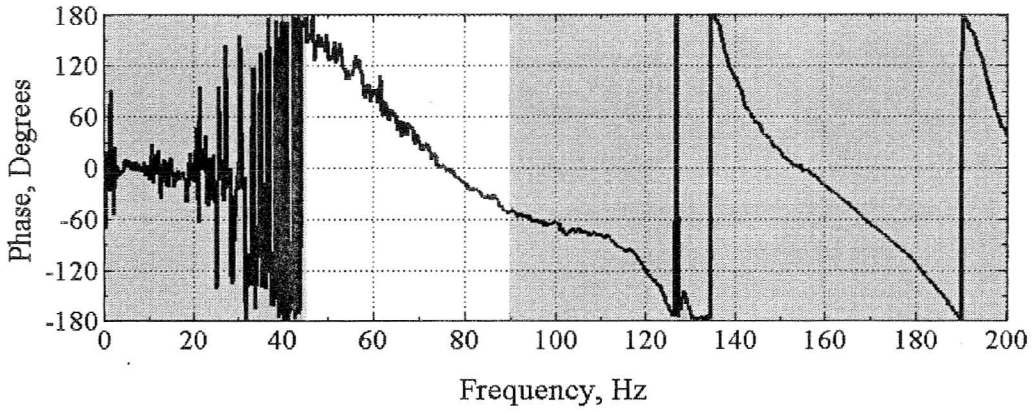

Figure X.7 Phase Plots Measured by SASW Testing with 6-ft Receiver Spacing (4E3_F_43.DAT)

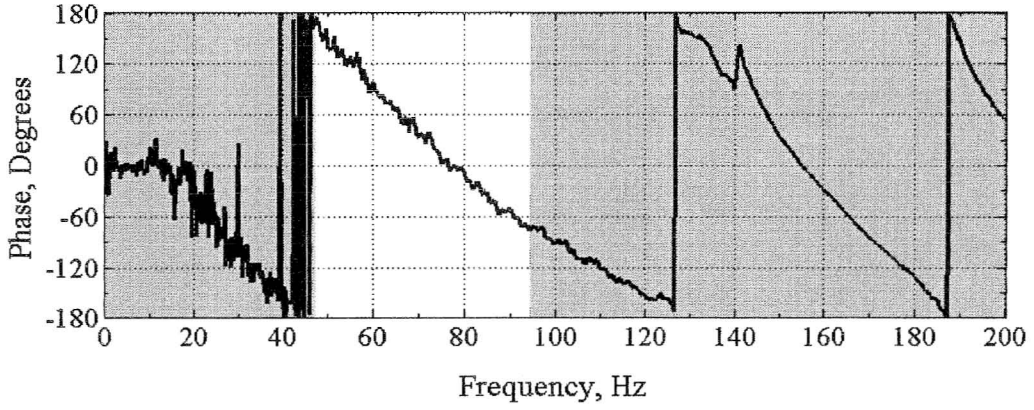

Figure X.8 Phase Plots Measured by SASW Testing with 6-ft Receiver Spacing (4E4_F_43.DAT)

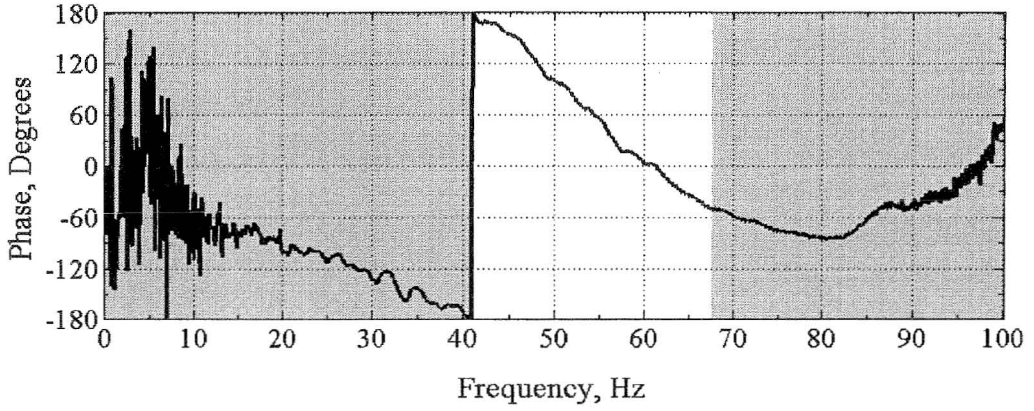

Figure X.9 Phase Plots Measured by SASW Testing with 9-ft Receiver Spacing (4E1_F_21.DAT)

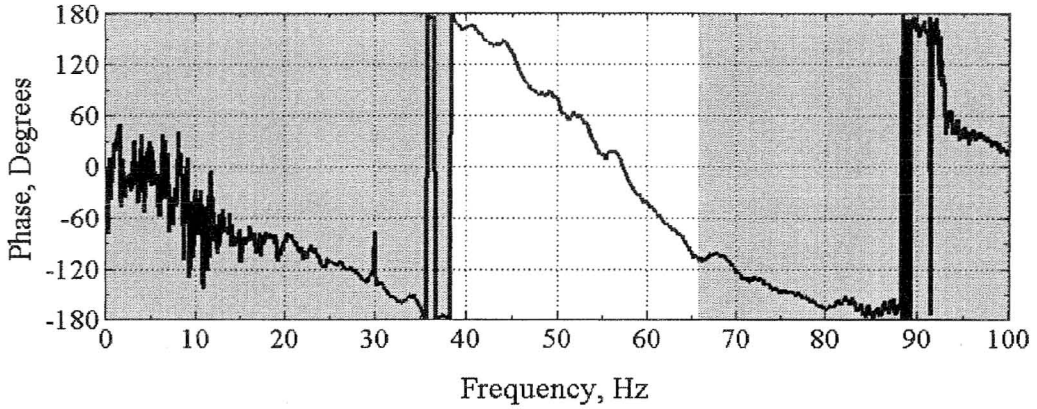

Figure X.10 Phase Plots Measured by SASW Testing with 9-ft Receiver Spacing (4E2_F_21.DAT)

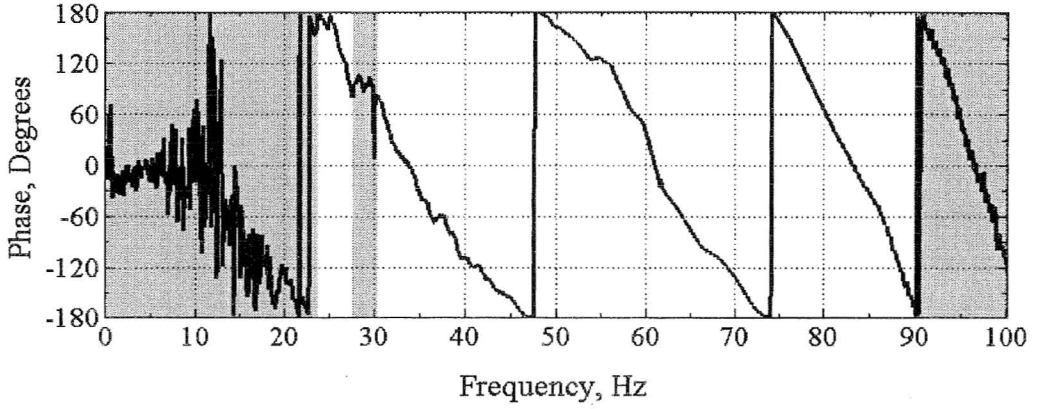

Figure X.11 Phase Plots Measured by SASW Testing with 18-ft Receiver Spacing (4E1_F_43.DAT)

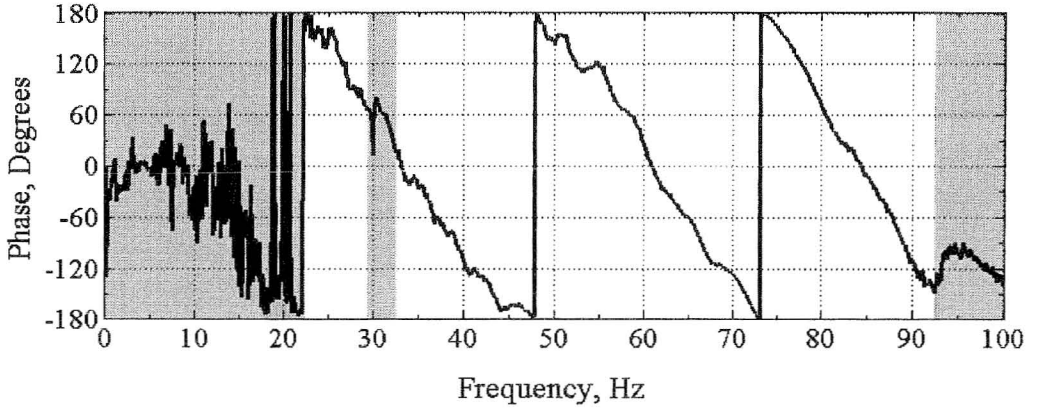

Figure X.12 Phase Plots Measured by SASW Testing with 18-ft Receiver Spacing (4E2_F_43.DAT)

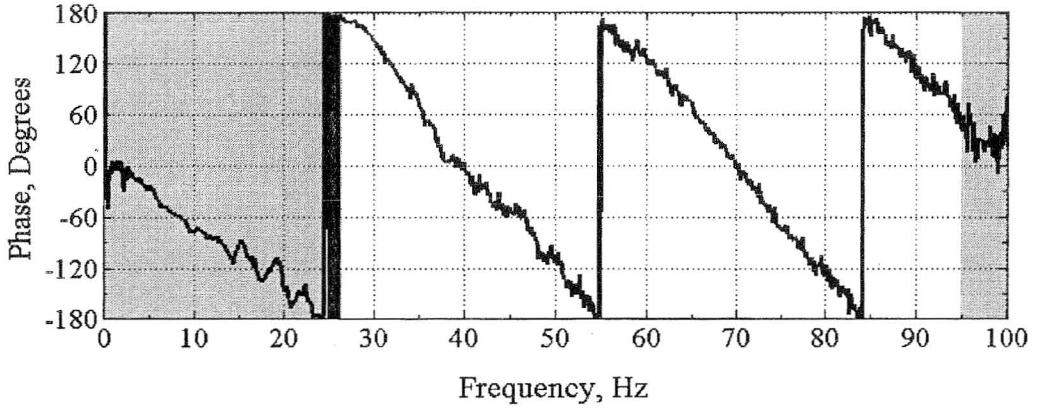

Figure X.13 Phase Plots Measured by SASW Testing with 15-ft Receiver Spacing (4G1_F_21.DAT)

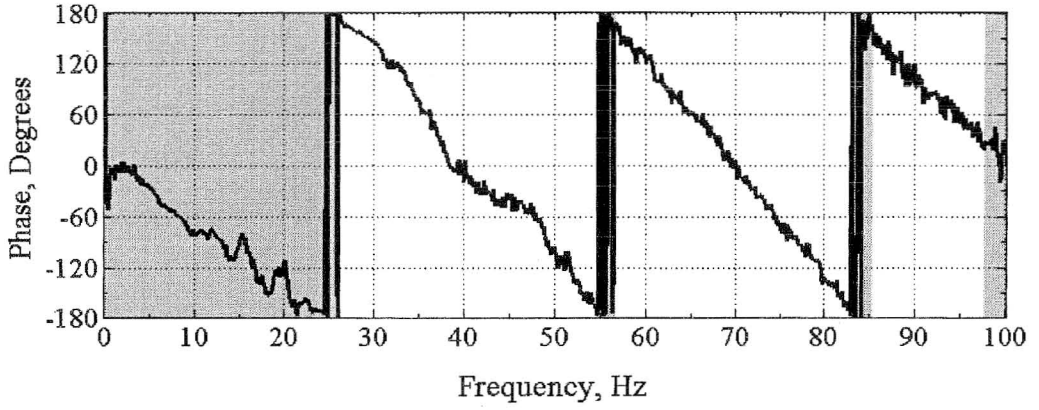

Figure X.14 Phase Plots Measured by SASW Testing with 15-ft Receiver Spacing (4G2_F_21.DAT)

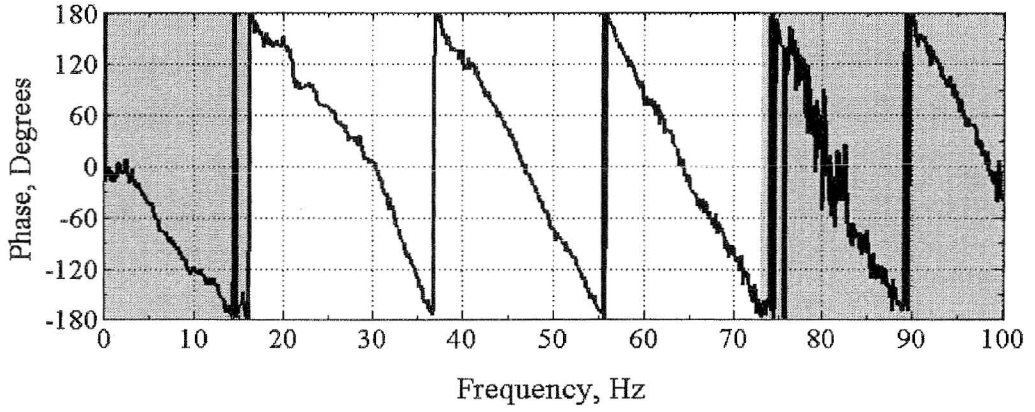

Figure X.15 Phase Plots Measured by SASW Testing with 25-ft Receiver Spacing (4G3_F_21.DAT)

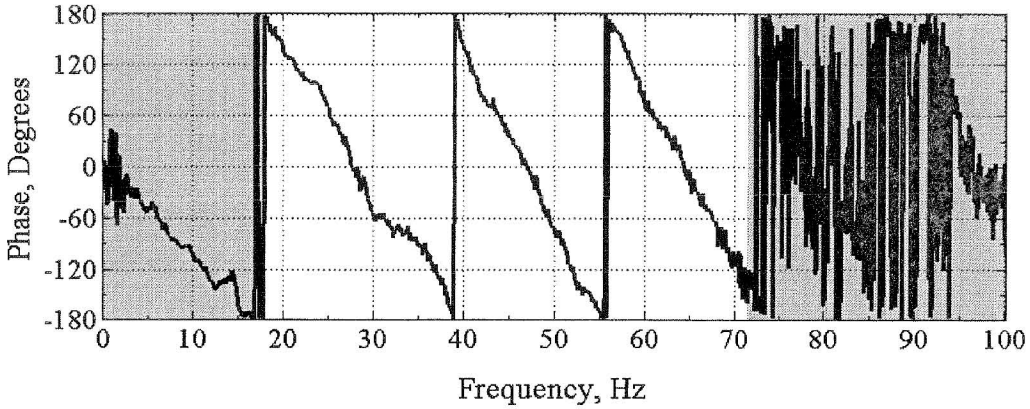

Figure X.16 Phase Plots Measured by SASW Testing with 25-ft Receiver Spacing (4G3_F_43.DAT)

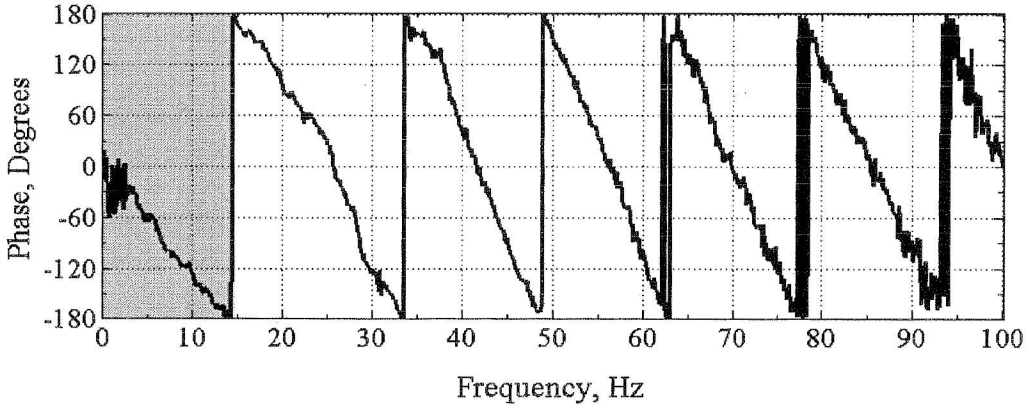

Figure X.17 Phase Plots Measured by SASW Testing with 30-ft Receiver Spacing (4G1_F_43.DAT)

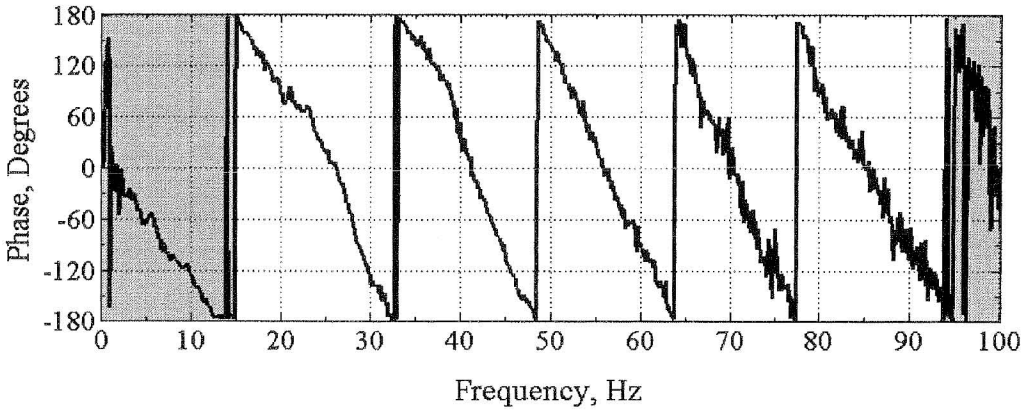

Figure X.18 Phase Plots Measured by SASW Testing with 30-ft Receiver Spacing (4G2_F_43.DAT)

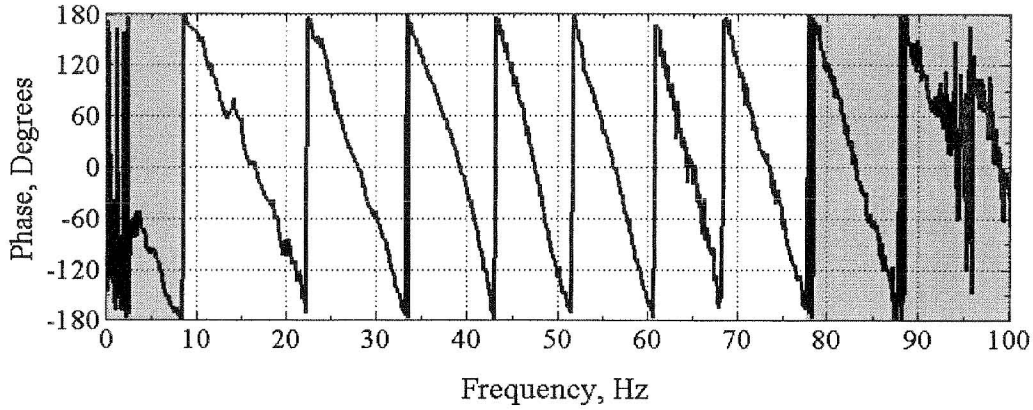

Figure X.19 Phase Plots Measured by SASW Testing with 50-ft Receiver Spacing (4G4_F_21.DAT)

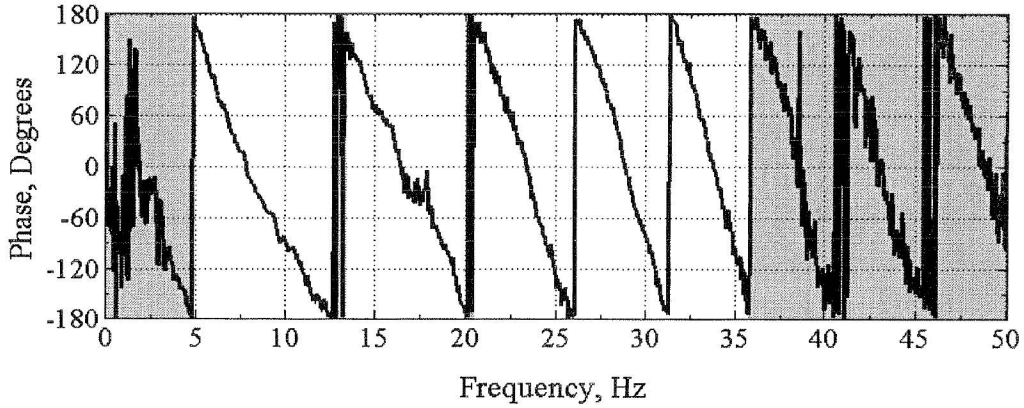

Figure X.20 Phase Plots Measured by SASW Testing with 100-ft Receiver Spacing (4G5_F_21.DAT)

Table X.1 Tables of Masking Parameters Used on Data Collected during Fourth Site Visit at Site E

Receiver Spacing (ft)	Masking Interval	Masking Start Frequency, Hz	Masking Stop Frequency, Hz	Number of Jumps	Filename
1	1	0	190	1	4E5_F_21.DAT
	2	402	800	-	
1	1	0	199	1	4E6_F_21.DAT
	2	416	800	-	
2	1	0	119	1	4E5_F_43.DAT
	2	137	151	1	
	3	398	800	-	
2	1	0	107	1	4E6_F_43.DAT
	2	390	800	-	
3	1	0	76.5	1	4E3_F_21.DAT
	2	118	200	-	
3	1	0	81.25	1	4E4_F_21.DAT
	2	126.5	200	-	
6	1	0	45.25	1	4E3_F_43.DAT
	2	89.5	200	-	
6	1	0	47.25	1	4E4_F_43.DAT
	2	94.25	200	-	
9	1	0	41	1	4E1_F_21.DAT
	2	67.62	100	-	
9	1	0	38.38	1	4E2_F_21.DAT
	2	65.75	100	-	
18	1	0	23.75	1	4E1_F_43.DAT
	2	27.62	30.38	2	
	3	89.62	100	-	
18	1	0	22.5	1	4E2_F_43.DAT
	2	29.38	32.62	1	
	3	92.25	100	-	
15	1	0	26.38	1	4G1_F_21.DAT
	2	94.75	100	-	
15	1	0	26.25	1	4G2_F_21.DAT
	2	54.62	56.62	2	
	3	82.75	85.12	3	
	4	97.38	100	-	

Performed by Jiabei Yuan Jiabei Yuan Checked by Yin-Cheng Lin Yin-Cheng Lin

Table X.2 Tables of Masking Parameters Used on Data Collected during Fourth Site Visit at Site E (Continued)

Receiver Spacing (ft)	Masking Interval	Masking Start Frequency, Hz	Masking Stop Frequency, Hz	Number of Jumps	Filename
25	1	0	16.25	1	4G3_F_21.DAT
	2	73	100	-	
25	1	0	18	1	4G3_F_43.DAT
	2	55.38	56	3	
	3	71.38	100	-	
30	1	0	14.62	1	4G1_F_43.DAT
30	1	0	15	1	4G2_F_43.DAT
	2	32.5	33.25	2	
	3	93.5	100	-	
50	1	0	8.62	1	4G4_F_21.DAT
	2	33.25	33.75	3	
	3	77.5	100	-	
100	1	0	4.88	1	4G5_F_21.DAT
	2	12.69	13.44	2	
	3	20.06	20.5	3	
	4	35.69	50	-	

Performed by Jiabei Yuan Checked by Yin-Cheng Lin

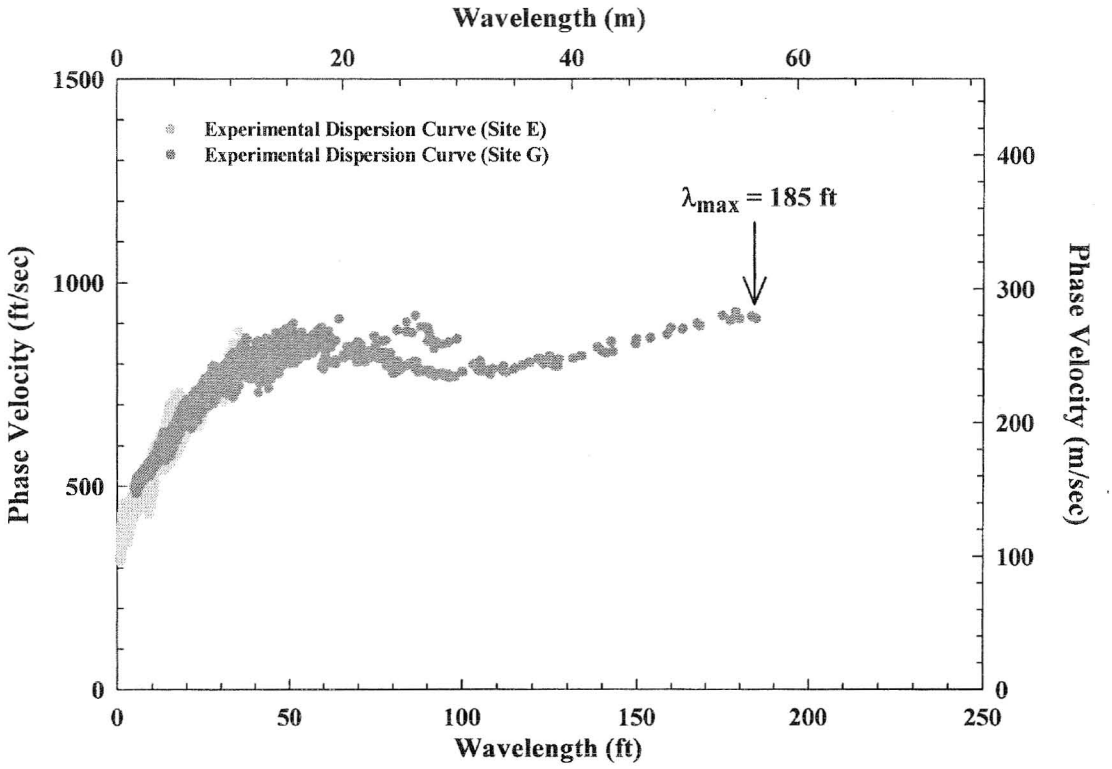

Figure X.21 Experimental Dispersion Curve Measured during Fourth Site Visit at Site E at Vogtle, GA; Linear Wavelength Axis

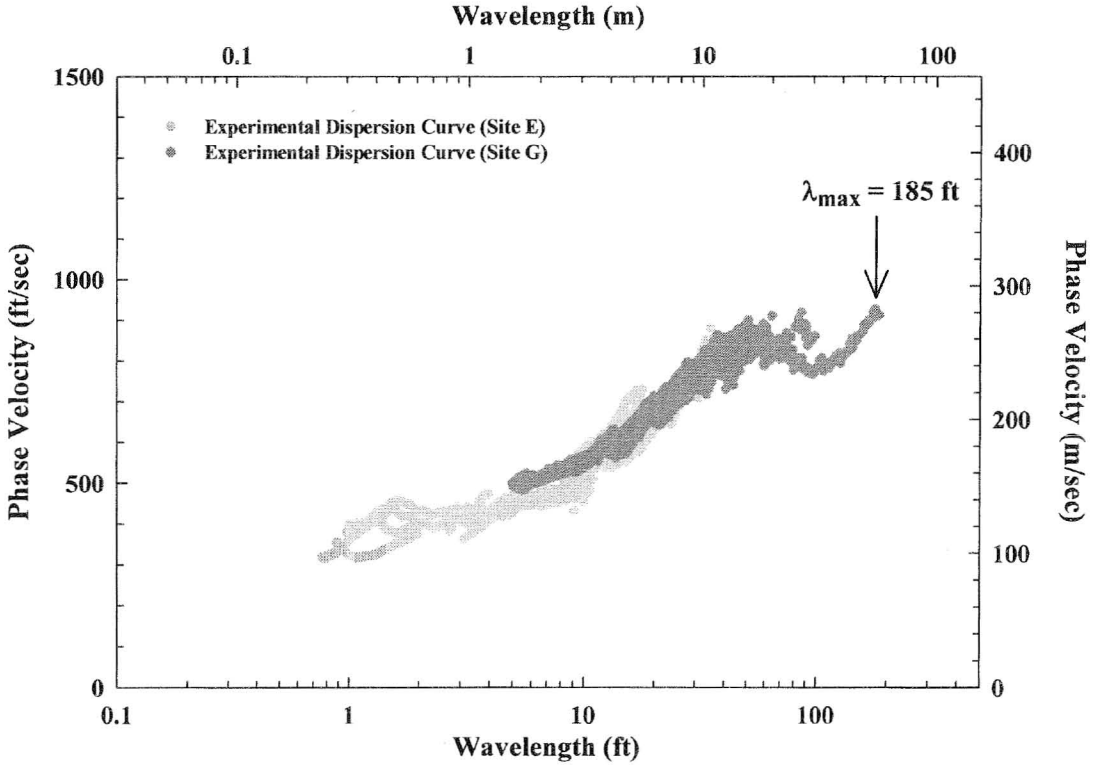

Figure X.22 Experimental Dispersion Curve Measured during Fourth Site Visit at Site E at Vogtle, GA; Logarithmic Wavelength Axis

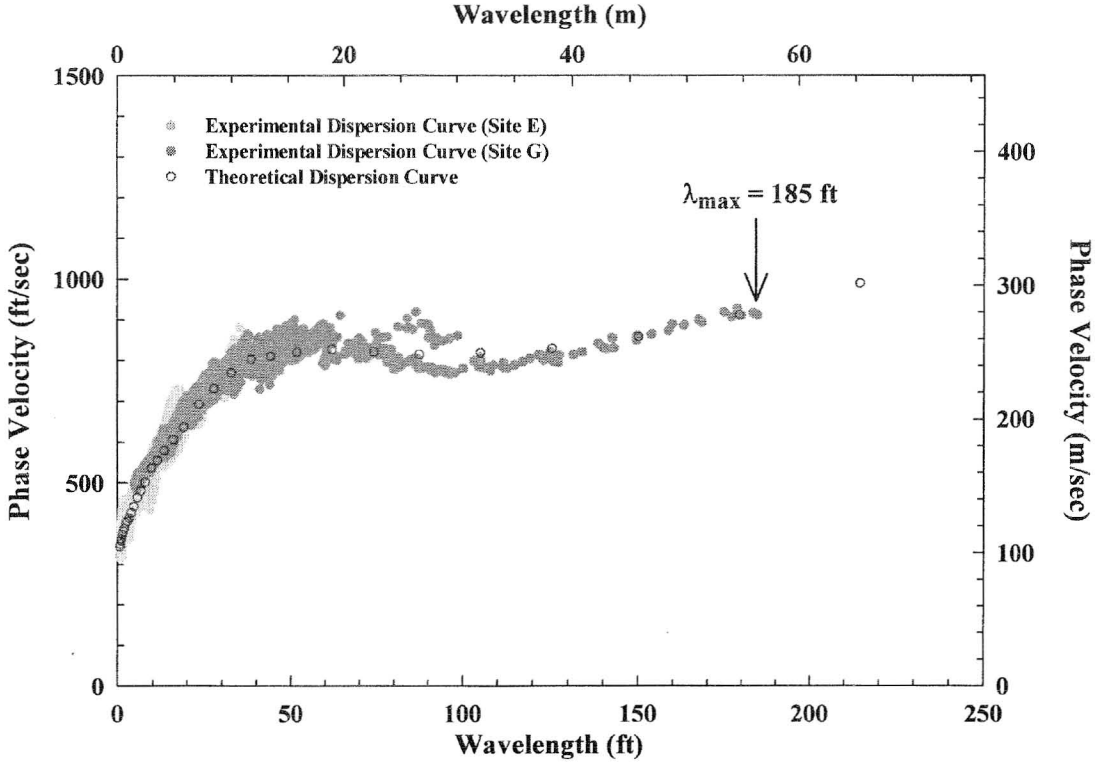

Figure X.23 Experimental and Theoretical Dispersion Curves from Site E in Fourth Site Visit at Vogtle, GA; Linear Wavelength Axis

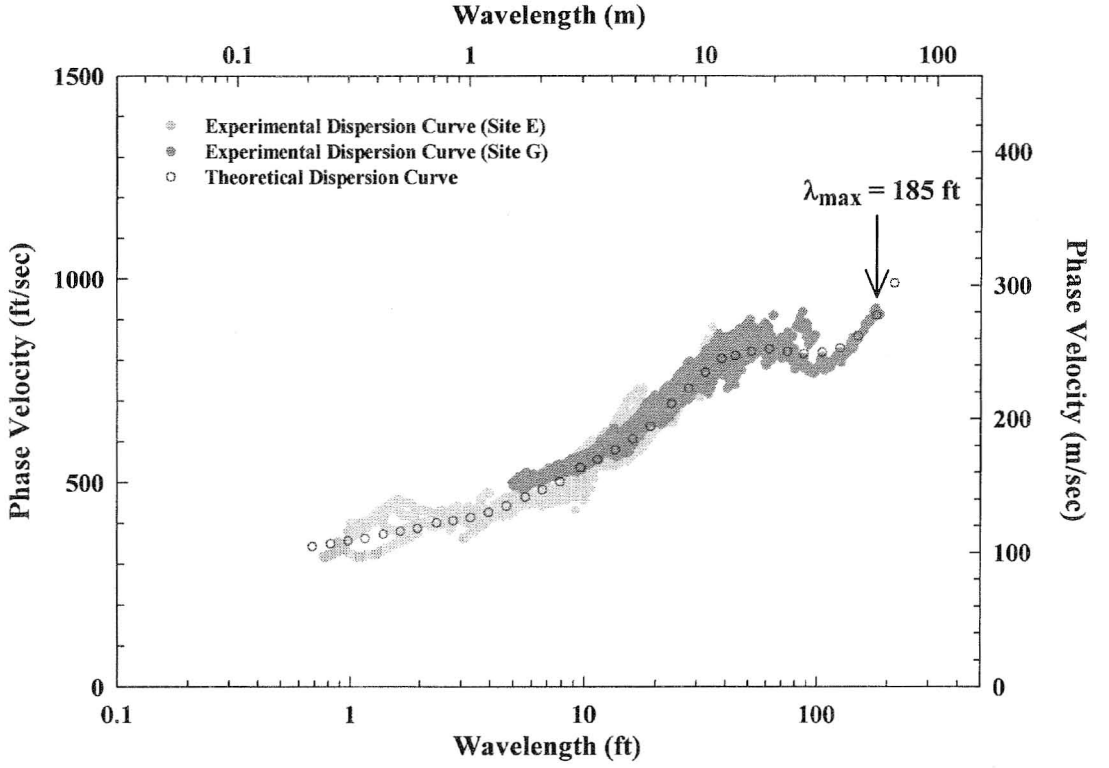

Figure X.24 Experimental and Theoretical Dispersion Curves from Site E in Fourth Site Visit at Vogtle, GA; Logarithmic Wavelength Axis

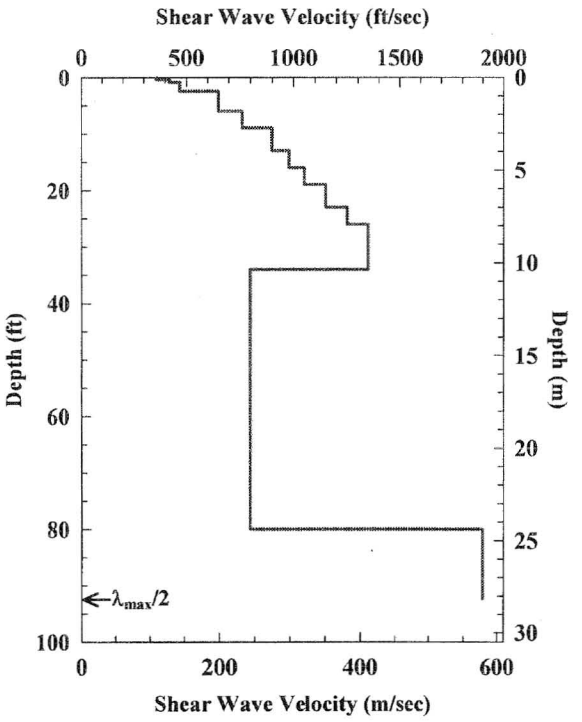

Figure X.25 Shear Wave Velocity Profile Determined at Site E during Fourth Site Visit at Vogtle, GA

Table X.3 Profile Parameters Used to Develop Preliminary Theoretical Dispersion Curve at Site E in the Fourth Site Visit at Vogtle, GA

Layer No.	Thickness, ft	Depth to Top of Layer, ft	S-Wave Velocity, ft/s	Assumed Poisson's Ratio	P-Wave Velocity, ft/s	Assumed Total Unit Weight, pcf
1	0.4	0.0	360	0.24	616	128
2	0.5	0.4	420	0.24	718	128
3	1.6	0.9	470	0.24	804	128
4	3.5	2.5	650	0.24	1111	128
5	3.0	6.0	760	0.24	1299	128
6	4.0	9.0	900	0.24	1539	128
7	3.0	13.0	980	0.24	1676	128
8	3.0	16.0	1050	0.24	1795	128
9	4.0	19.0	1150	0.24	1966	128
10	3.0	23.0	1250	0.24	2137	128
11	8.0	26.0	1350	0.24	2308	128
12	46.0	34.0	800	0.24	1368	128
13#	12.3	80.0	1900	0.42	5000	135
14*#	17.7	92.3	2200	0.38	5000	135
15*#	Half Space	110.0	2200	0.38	5000	135

* Layer below maximum depth of the V_S Profile.

\# Layer below water tatble.

Performed by Yin-Cheng Lin Yin-Cheng Lin Checked by K. H. Stokoe, II Kenneth H. Stokoe, II

Appendix Y

SASW Measurements of Fourth Site Visit at Vogtle, GA
Site Location: Site F

3 - Receiver SASW Data Sheet

Page ___ of ___

Project : Vogtle

Data Sheet # : SA4#6

Location : F(SA4#6)

Disk # : SA4#6

Date/(Time) : Jan / 24 / 2008 : ~ :)

Personnel : Stokoe, Tuan, Minjae

Recorded by : Tuan

Checked by : Minjae

R1 I.D. : UT07-4.5H2-04, GT(92003

R2 I.D. : UT07-4.5H8-02, GT(92002

R3 I.D. : UT07-4.5H2-03, GT(92001

Sketch

Distance (ft)			Impact Direction		Impact Source	Record #	Freq. Range (Hz)	Notes
S - R1	R1 - R2	R2 - R3						
1	1	2	(For)	Rev	Sledge Hammer	4F1	0 - 800	hammer on plate, soft hit
1	1	2	For	(Rev)	"	4F2	0 - 800	" " "
2	2	4	For	(Rev)	med "	4F3	0 - 200	"
3	3	6	(For)	Rev	"	4F4	0 - 200	"
9	9	18	(For)	Rev	sledge hammer	4F5	0 - 100	"
9	9	18	For	(Rev)	"	4F6	0 - 100	"
			For	Rev			~	
			For	Rev			~	
			For	Rev			~	
			For	Rev			~	
			For	Rev			~	
			For	Rev			~	
			For	Rev			~	
			For	Rev			~	
			For	Rev			~	
			For	Rev			~	

* Autosequence 3R_SASW saves F_2/1, C_2/1, F_4/3, C_4/3, Lin_1, Lin_2, Lin_4

* Autosequence 3R_SEWPSIN saves F_2/1, Var_2, F_4/3, Var_4, Lin_1, Lin_2, Lin_4

University of Texas at Austin

3 - Receiver SASW Data Sheet

Page ___ of ___

Project : Vogtle

Data Sheet # : SA4 #7

Location : G7 (SA4 #7)

Disk # : SA4 #7

Date/(Time) : Jan / 24 / 2008 (: ~ :)

Personnel : Stokoe, Tuan, Minjae

Recorded by : Tuan

Checked by : Minjae

R1 I.D. : UT07 - 4.5Hz -04, GBC92003

R2 I.D. : UT07 - 4.5Hz -03, GBC92002

R3 I.D. : UT07 - 4.5Hz -03, GBC92001

Sketch

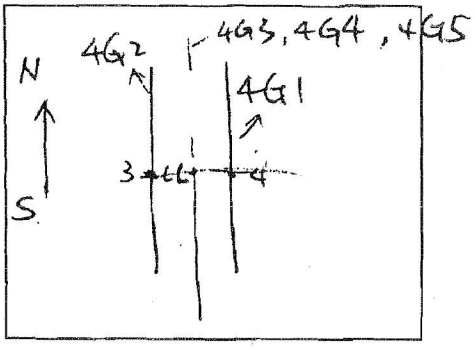

Distance (ft)			Impact Direction		Impact Source	Record #	Freq. Range (Hz)	Notes
S - R1	R1 - R2	R2 - R3						
15	15	30	For	~~Rev~~	bulldozer	4G1	0 - 100	
15	15	30	For	~~Rev~~	"	4G2	0 - 100	
25	25	25	For	~~Rev~~	"	4G3	0 - 100	
50	50	—	For	~~Rev~~	"	4G4	0 - 100	
100	100	—	For	~~Rev~~	"	4G5	0 - 50	
			For	Rev			~	
			For	Rev			~	
			For	Rev			~	
			For	Rev			~	
			For	Rev			~	
			For	Rev			~	
			For	Rev			~	
			For	Rev			~	
			For	Rev			~	
			For	Rev			~	
			For	Rev			~	

* Autosequence 3R_SASW saves F_2/1, C_2/1, F_4/3, C_4/3, Lin_1, Lin_2, Lin_4

* Autosequence 3R_SEWPSIN saves F_2/1, Var_2, F_4/3, Var_4, Lin_1, Lin_2, Lin_4

University of Texas at Austin

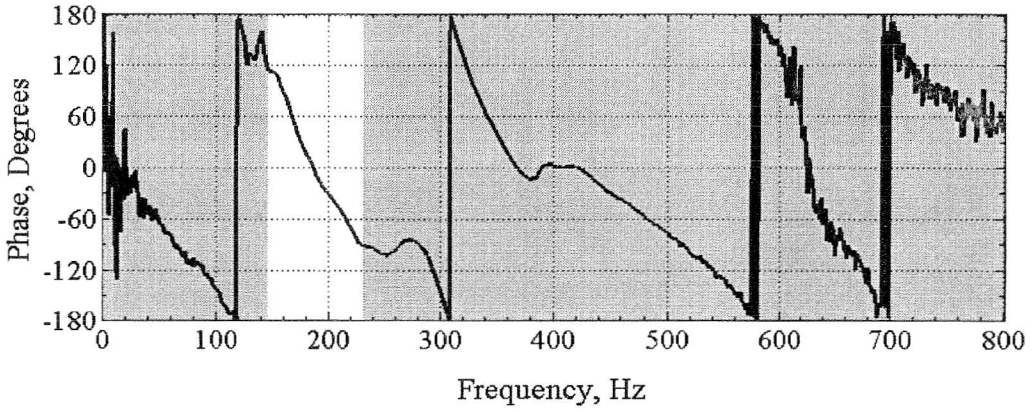

Figure Y.1 Phase Plots Measured by SASW Testing with 2-ft Receiver Spacing (4F1_F_43.DAT)

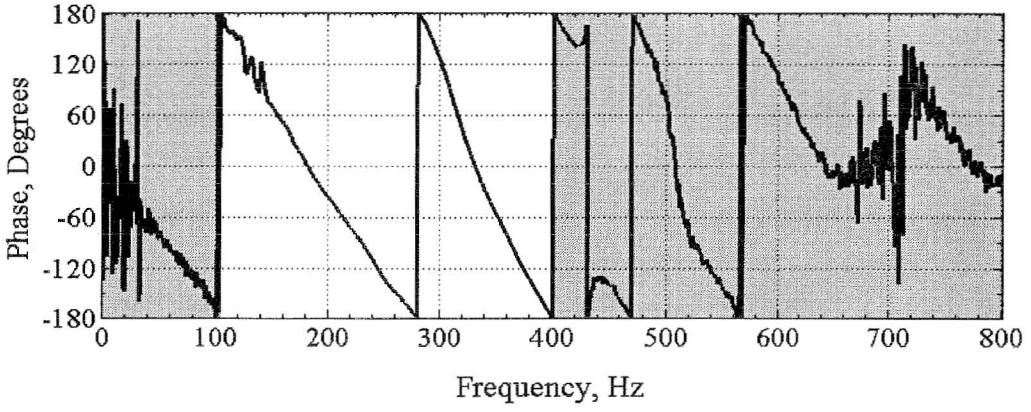

Figure Y.2 Phase Plots Measured by SASW Testing with 2-ft Receiver Spacing (4F2_F_43.DAT)

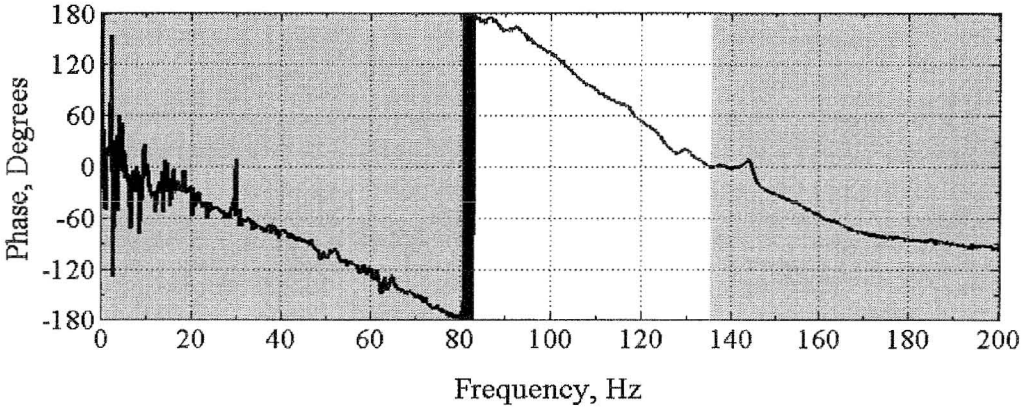

Figure Y.3 Phase Plots Measured by SASW Testing with 3-ft Receiver Spacing (4F3_F_21.DAT)

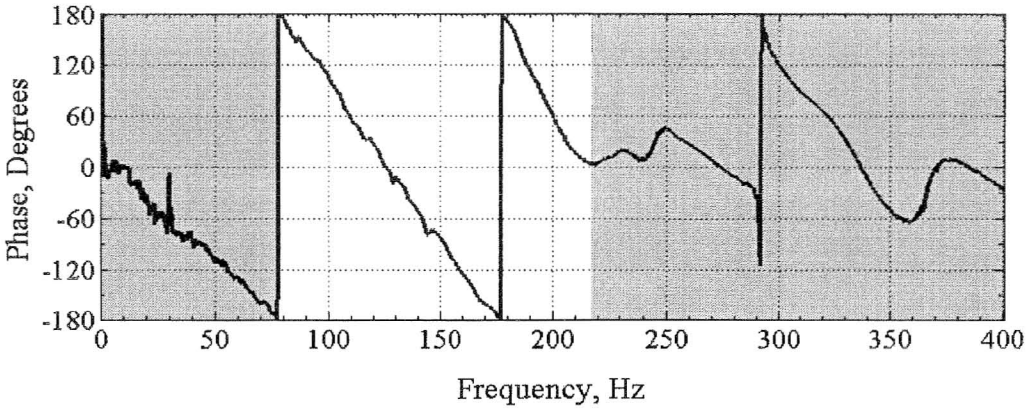

Figure Y.4 Phase Plots Measured by SASW Testing with 3-ft Receiver Spacing (4F4_F_21.DAT)

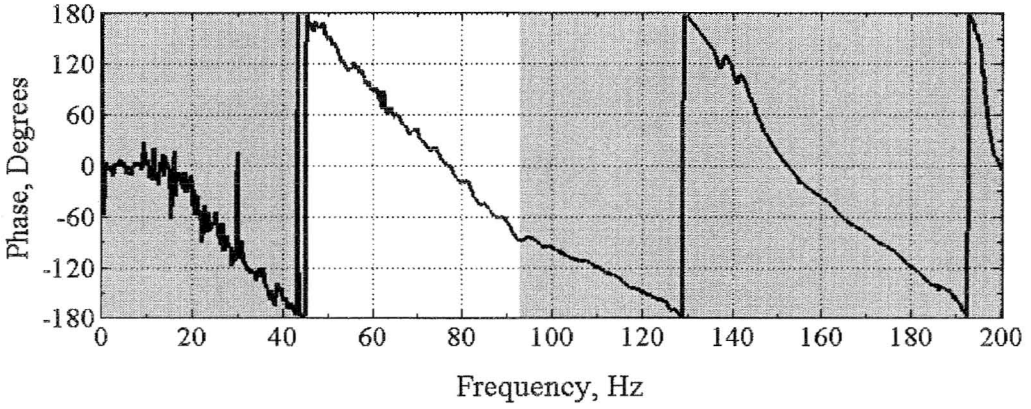

Figure Y.5 Phase Plots Measured by SASW Testing with 6-ft Receiver Spacing (4F3_F_43.DAT)

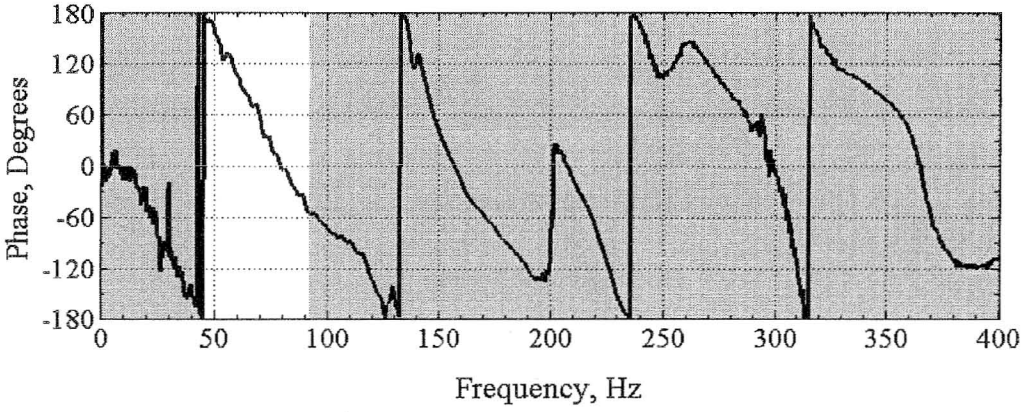

Figure Y.6 Phase Plots Measured by SASW Testing with 6-ft Receiver Spacing (4F4_F_43.DAT)

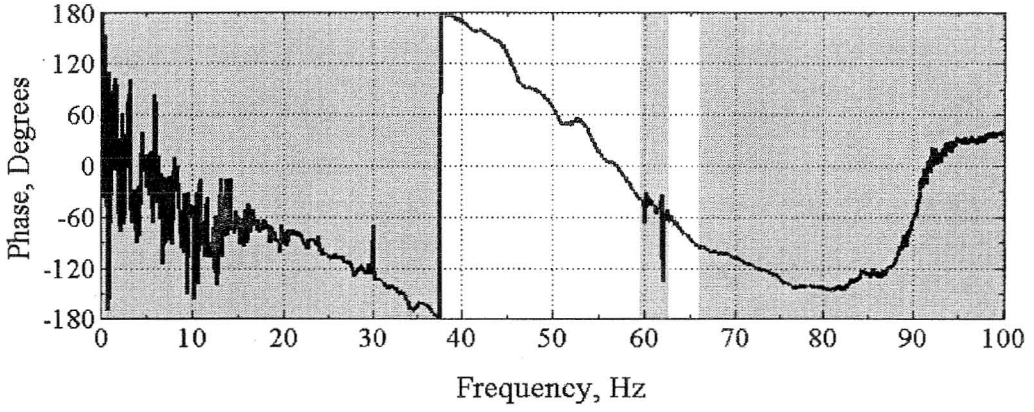

Figure Y.7 Phase Plots Measured by SASW Testing with 9-ft Receiver Spacing (4F5_F_21.DAT)

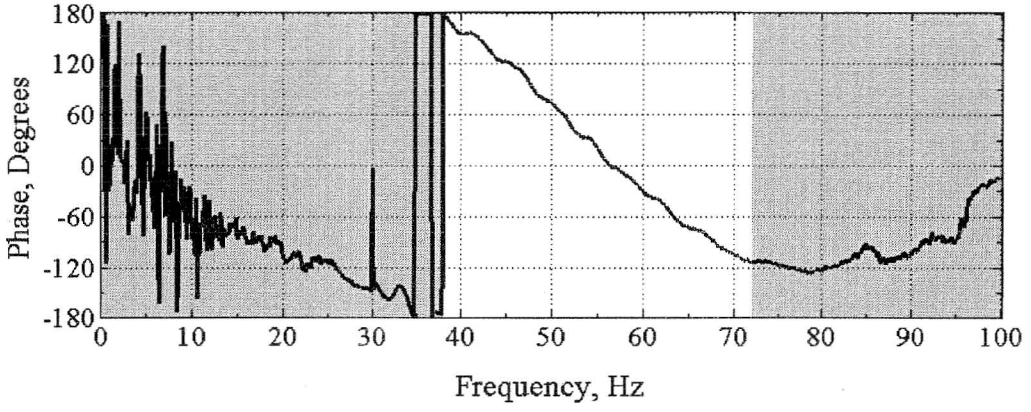

Figure Y.8 Phase Plots Measured by SASW Testing with 9-ft Receiver Spacing (4F6_F_21.DAT)

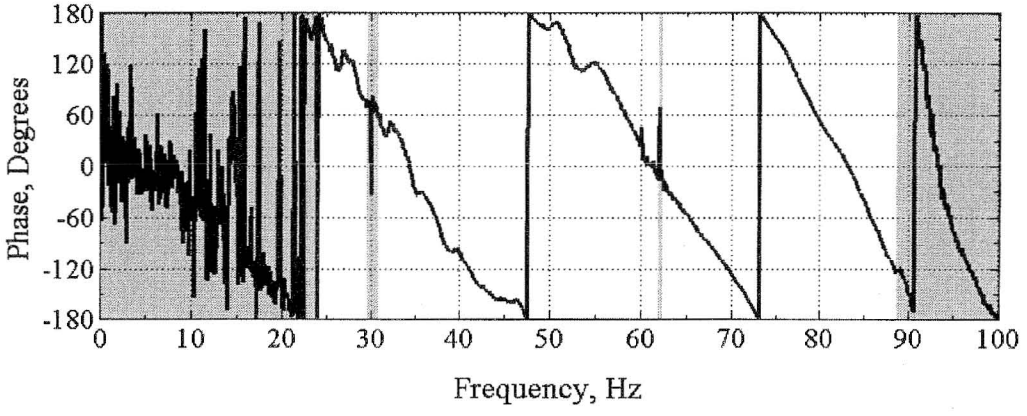

Figure Y.9 Phase Plots Measured by SASW Testing with 18-ft Receiver Spacing (4F5_F_43.DAT)

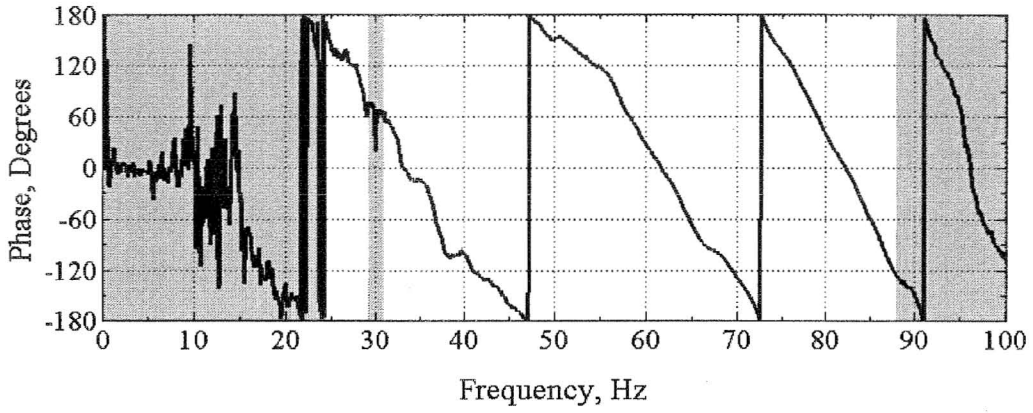

Figure Y.10 Phase Plots Measured by SASW Testing with 18-ft Receiver Spacing (4F6_F_43.DAT)

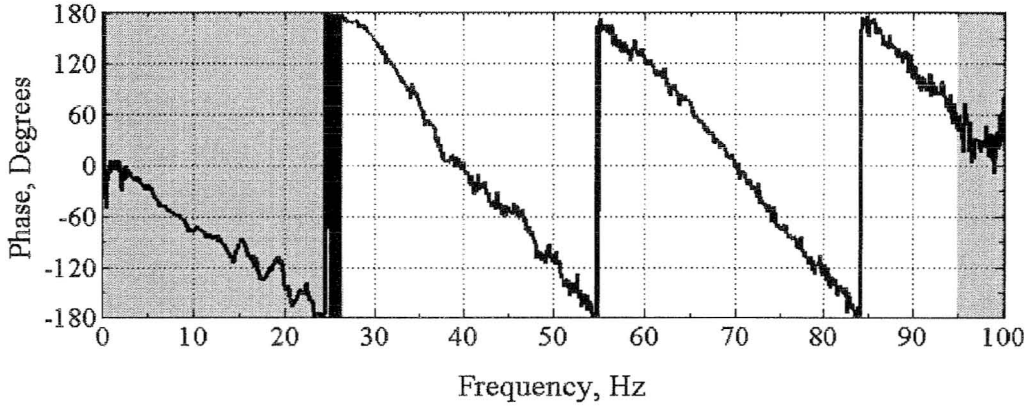

Figure Y.11 Phase Plots Measured by SASW Testing with 15-ft Receiver Spacing (4G1_F_21.DAT)

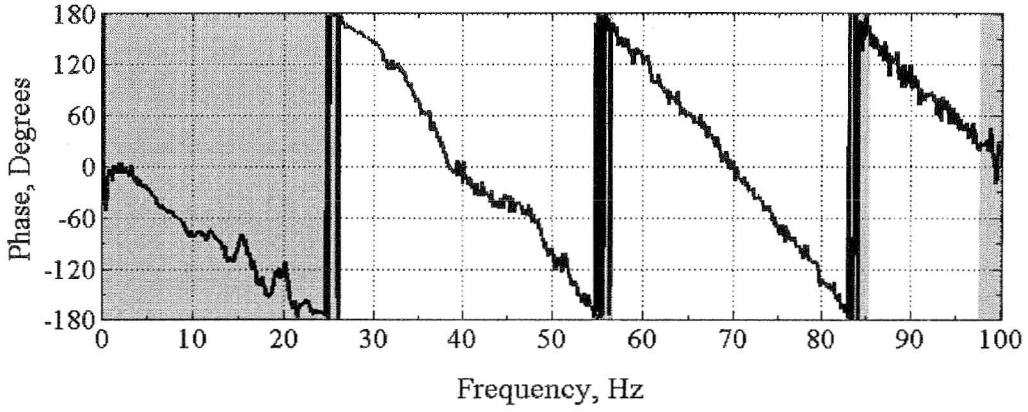

Figure Y.12 Phase Plots Measured by SASW Testing with 15-ft Receiver Spacing (4G2_F_21.DAT)

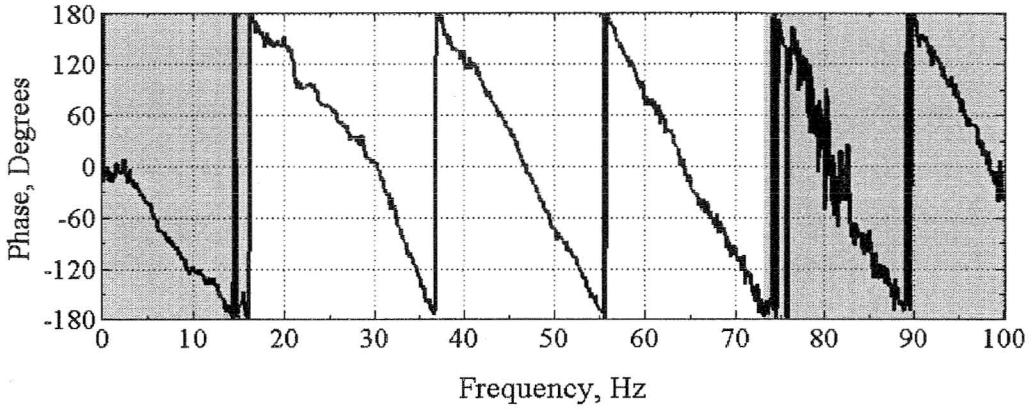

Figure Y.13 Phase Plots Measured by SASW Testing with 25-ft Receiver Spacing (4G3_F_21.DAT)

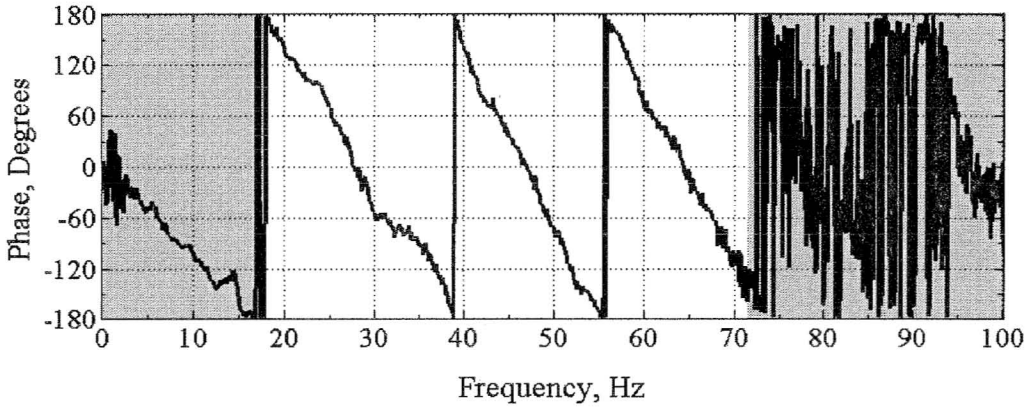

Figure Y.14 Phase Plots Measured by SASW Testing with 25-ft Receiver Spacing (4G3_F_43.DAT)

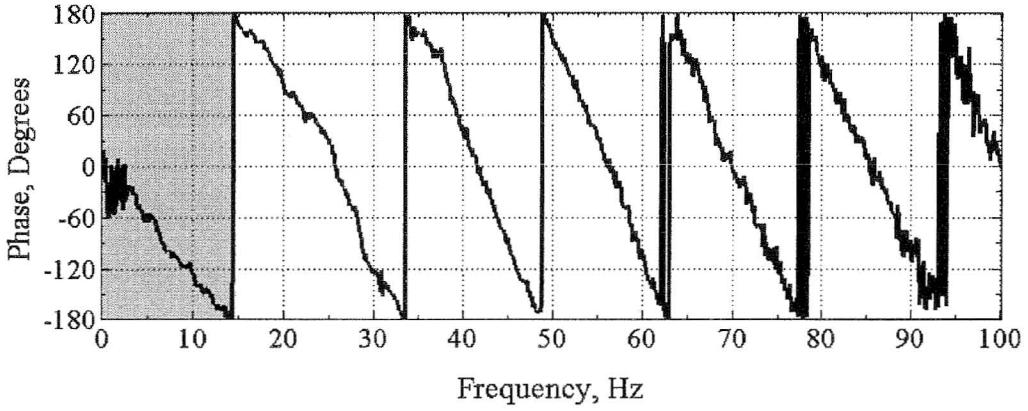

Figure Y.15 Phase Plots Measured by SASW Testing with 30-ft Receiver Spacing (4G1_F_43.DAT)

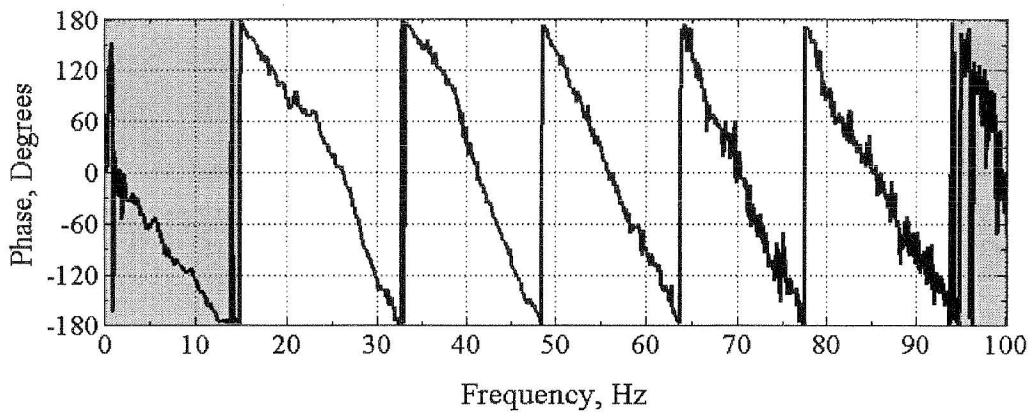

Figure Y.16 Phase Plots Measured by SASW Testing with 30-ft Receiver Spacing (4G2_F_43.DAT)

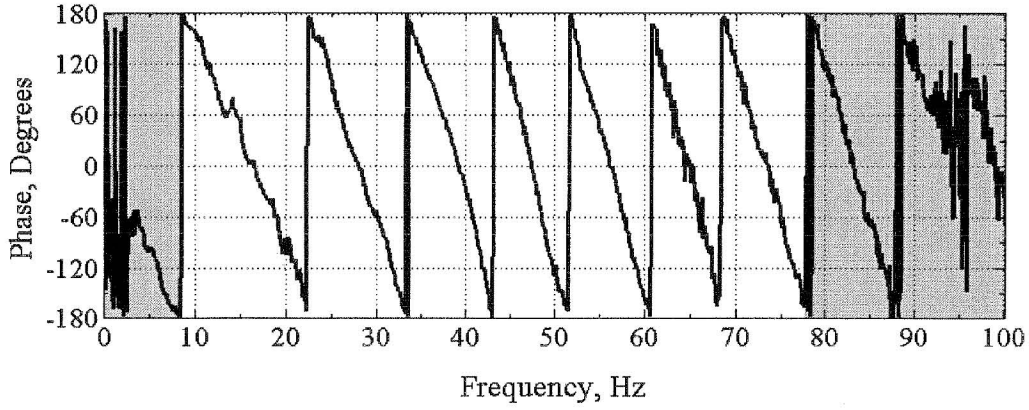

Figure Y.17 Phase Plots Measured by SASW Testing with 50-ft Receiver Spacing (4G4_F_21.DAT)

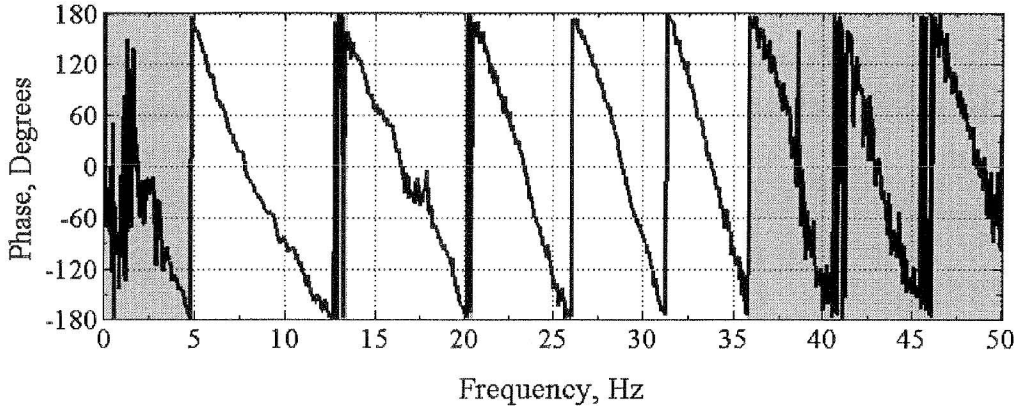

Figure Y.18 Phase Plots Measured by SASW Testing with 100-ft Receiver Spacing (4G5_F_21.DAT)

Table Y.1 Tables of Masking Parameters Used on Data Collected during Fourth Site Visit at Site F

Receiver Spacing (ft)	Masking Interval	Masking Start Frequency, Hz	Masking Stop Frequency, Hz	Number of Jumps	Filename
2	1	0	146	1	4F1_F_43.DAT
	2	231	800	-	
2	1	0	106	1	4F2_F_43.DAT
	2	400	800	-	
3	1	0	83	1	4F3_F_21.DAT
	2	135.5	200	-	
3	1	0	78	1	4F4_F_21.DAT
	2	216.5	400	-	
6	1	0	45.25	1	4F3_F_43.DAT
	2	92.75	200	-	
6	1	0	45.5	1	4F4_F_43.DAT
	2	92.5	400	-	
9	1	0	37.62	1	4F5_F_21.DAT
	2	59.5	62.5	1	
	3	66	100	-	
9	1	0	38	1	4F6_F_21.DAT
	2	71.88	100	-	
18	1	0	24.12	1	4F5_F_43.DAT
	2	29.5	30.88	2	
	3	61.88	62.25	2	
	4	88.38	100	-	
18	1	0	24.38	1	4F6_F_43.DAT
	2	29.25	31	1	
	3	87.62	100	-	
15	1	0	26.38	1	4G1_F_21.DAT
	2	94.75	100	-	
15	1	0	26.25	1	4G2_F_21.DAT
	2	54.62	56.62	2	
	3	82.75	85.12	3	
	4	97.38	100	-	

Performed by Jiabei Yuan Checked by Yin-Cheng Lin

Table Y.2 Tables of Masking Parameters Used on Data Collected during Fourth Site Visit at Site F (Continued)

Receiver Spacing (ft)	Masking Interval	Masking Start Frequency, Hz	Masking Stop Frequency, Hz	Number of Jumps	Filename
25	1	0	16.25	1	4G3_F_21.DAT
	2	73	100	-	
25	1	0	18	1	4G3_F_43.DAT
	2	55.38	56	3	
	3	71.38	100	-	
30	1	0	14.62	1	4G1_F_43.DAT
30	1	0	15	1	4G2_F_43.DAT
	2	32.5	33.25	2	
	3	93.5	100	-	
50	1	0	8.62	1	4G4_F_21.DAT
	2	33.25	33.75	3	
	3	77.5	100	-	
100	1	0	4.88	1	4G5_F_21.DAT
	2	12.69	13.44	2	
	3	20.06	20.5	3	
	4	35.69	50	-	

Performed by Jiabei Yuan Jiabei Yuan Checked by Yin-Cheng Lin Yin-Cheng Lin

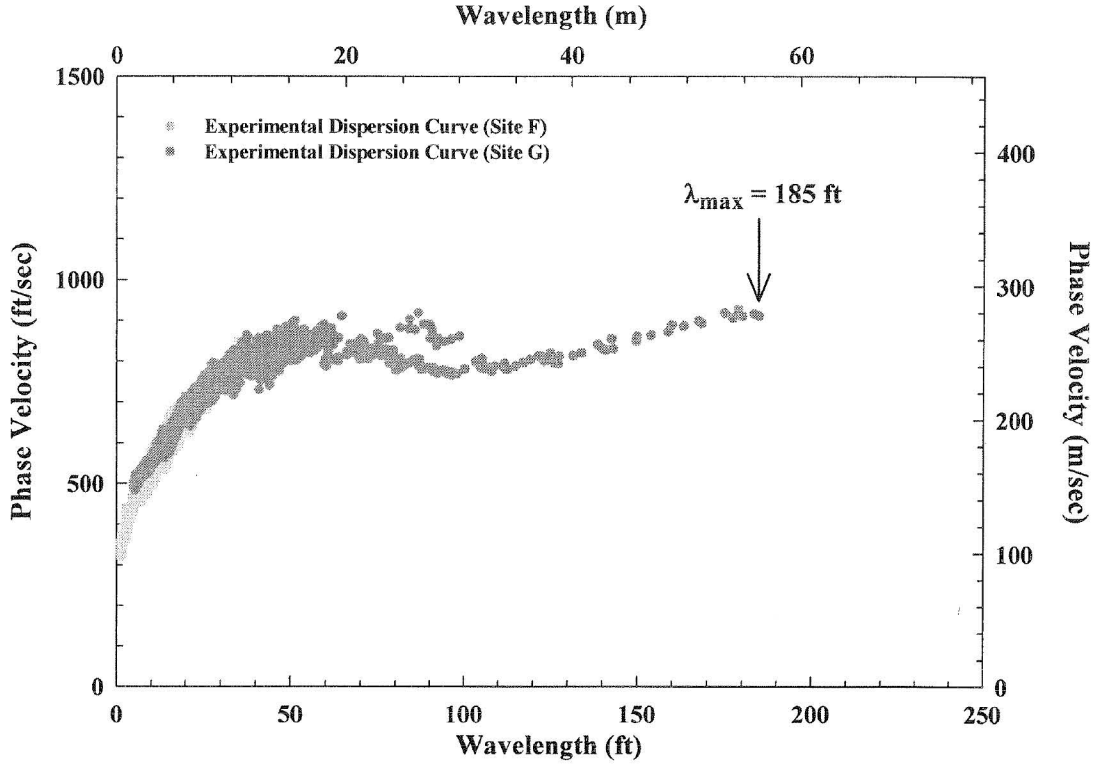

Figure Y.19 Experimental Dispersion Curve Measured during Fourth Site Visit at Site F at Vogtle, GA; Linear Wavelength Axis

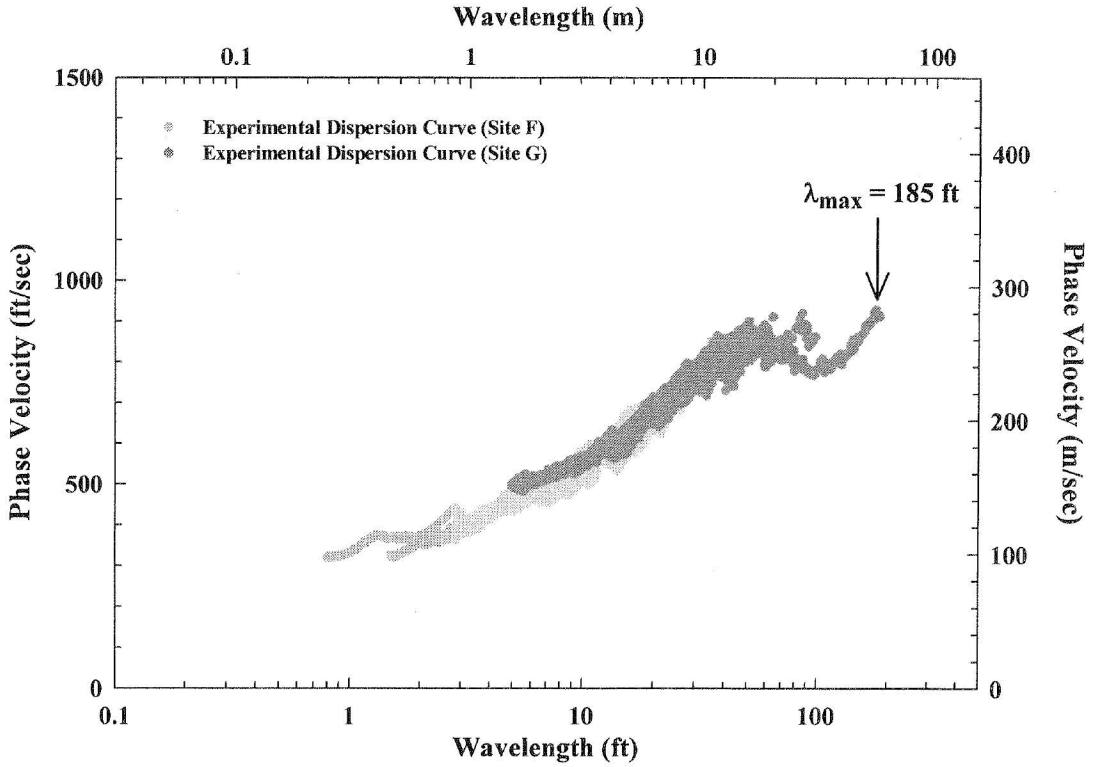

Figure Y.20 Experimental Dispersion Curve Measured during Fourth Site Visit at Site F at Vogtle, GA; Logarithmic Wavelength Axis

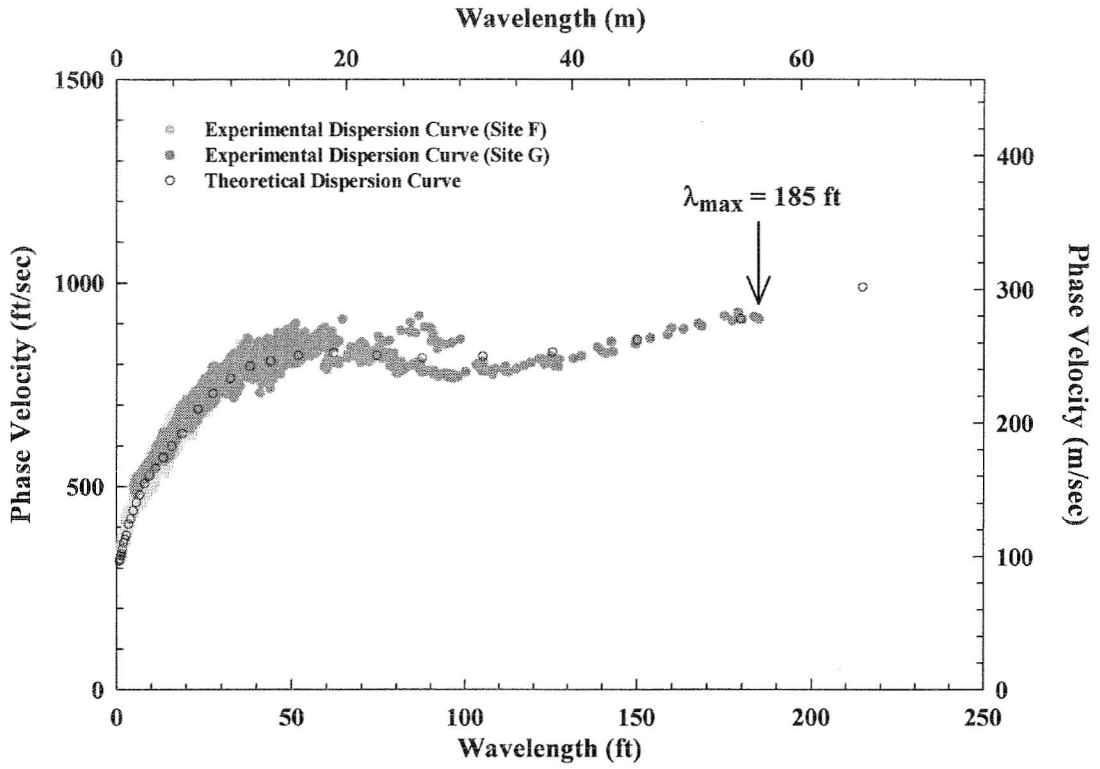

Figure Y.21 Experimental and Theoretical Dispersion Curves from Site F in Fourth Site Visit at Vogtle, GA; Linear Wavelength Axis

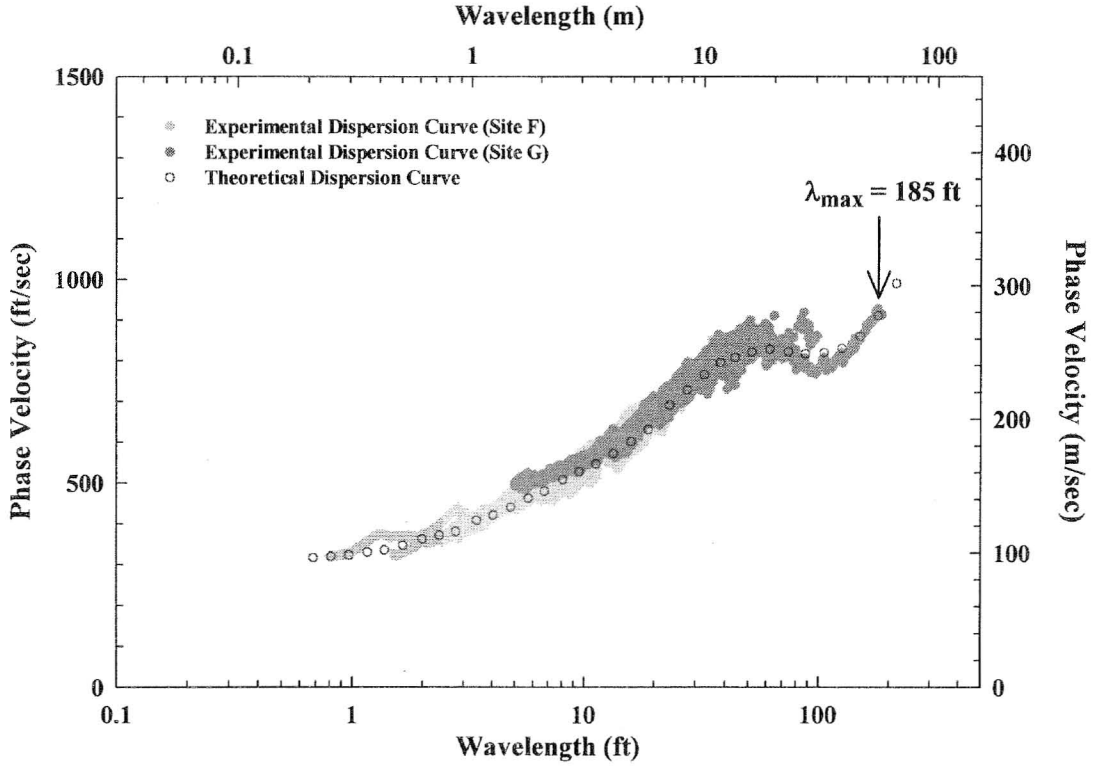

Figure Y.22 Experimental and Theoretical Dispersion Curves from Site F in Fourth Site Visit at Vogtle, GA; Logarithmic Wavelength Axis

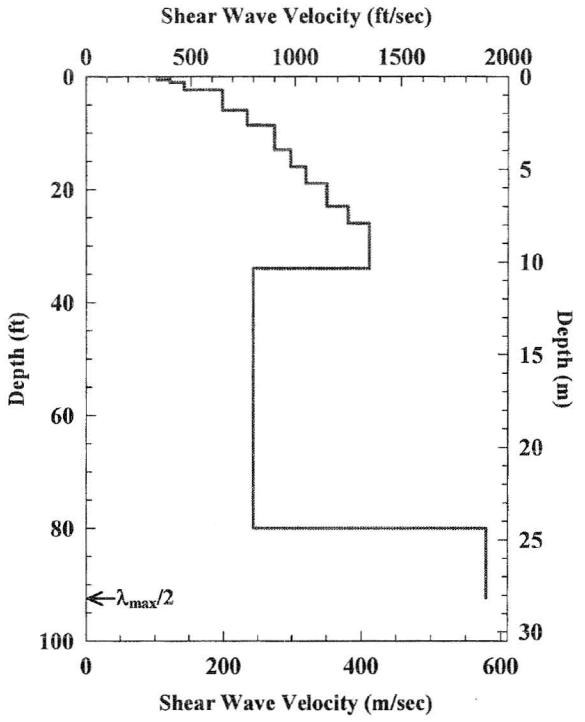

Figure Y.23 Shear Wave Velocity Profile Determined at Site F during Fourth Site Visit at Vogtle, GA

Table Y.3 Profile Parameters Used to Develop Preliminary Theoretical Dispersion Curve at Site F in the Fourth Site Visit at Vogtle, GA

Layer No.	Thickness, ft	Depth to Top of Layer, ft	S-Wave Velocity, ft/s	Assumed Poisson's Ratio	P-Wave Velocity, ft/s	Assumed Total Unit Weight, pcf
1	0.6	0.0	340	0.24	581	128
2	0.5	0.6	400	0.24	684	128
3	1.3	1.1	470	0.24	804	128
4	3.6	2.4	650	0.24	1111	128
5	2.7	6.0	770	0.24	1317	128
6	4.3	8.7	900	0.24	1539	128
7	3.0	13.0	980	0.24	1676	128
8	3.0	16.0	1050	0.24	1795	128
9	4.0	19.0	1150	0.24	1966	128
10	3.0	23.0	1250	0.24	2137	128
11	8.0	26.0	1350	0.24	2308	128
12	46.0	34.0	800	0.24	1368	128
13#	12.3	80.0	1900	0.42	5000	135
14*#	17.7	92.3	2200	0.38	5000	135
15*#	Half Space	110.0	2200	0.38	5000	135

* Layer below maximum depth of the V_S Profile.

\# Layer below water tatble.

Performed by Yin-Cheng Lin Checked by K. H. Stokoe

Yin-Cheng Lin Kenneth H. Stokoe, II

Appendix Z

SASW Measurements of Fourth Site Visit at Vogtle, GA
Site Location: Site H

3 - Receiver SASW Data Sheet

Page ___ of ___

Project : Vogtle

Data Sheet # : SA4#8

Location : H (SA4#8)

Disk # : SA4#8

Date/(Time) : / / (5:42PM ~ :)

Personnel : Stokoe Yuan Minjae

Recorded by : Yuan

Checked by : Minjae

R1 I.D. : UT07-4.5Hz-04, GBC92003

R2 I.D. : UT07-4.5Hz-02, GBC92002

R3 I.D. : UT07-4.5Hz-03, GBC92001

Sketch

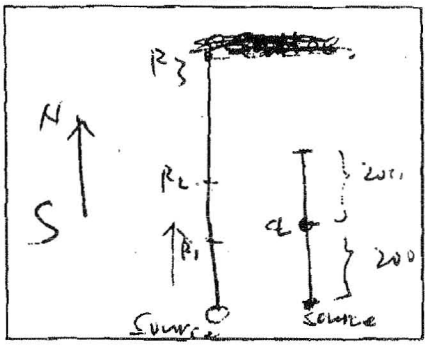

Distance (ft)			Impact Direction		Impact Source	Record #	Freq. Range (Hz)	Notes
S - R1	R1 - R2	R2 - R3						
25	25	50	For	Rev	Bull dozer	4H1	0 - 100	
25	25	25	For	Rev	"	4H2	0 - 100	
50	50	50	For	Rev	"	4H3	0 - 100	
100	100	100	For	Rev	"	4H4	0 - 50	
200	200		For	Rev	"	4H5	0 - 25	Save trace by hand
6	6	12	For	Rev	Med "	4H6	0 - 400	soft hit
6	6	12	For	Rev	"	4H7	0 - 400	"
			For	Rev			~	
			For	Rev			~	
			For	Rev			~	
			For	Rev			~	
			For	Rev			~	
			For	Rev			~	
			For	Rev			~	
			For	Rev			~	
			For	Rev			~	

* Autosequence 3R_SASW saves F_2/1, C_2/1, F_4/3, C_4/3, Lin_1, Lin_2, Lin_4

* Autosequence 3R_SEWPSIN saves F_2/1, Var_2, F_4/3, Var_4, Lin_1, Lin_2, Lin_4

University of Texas at Austin

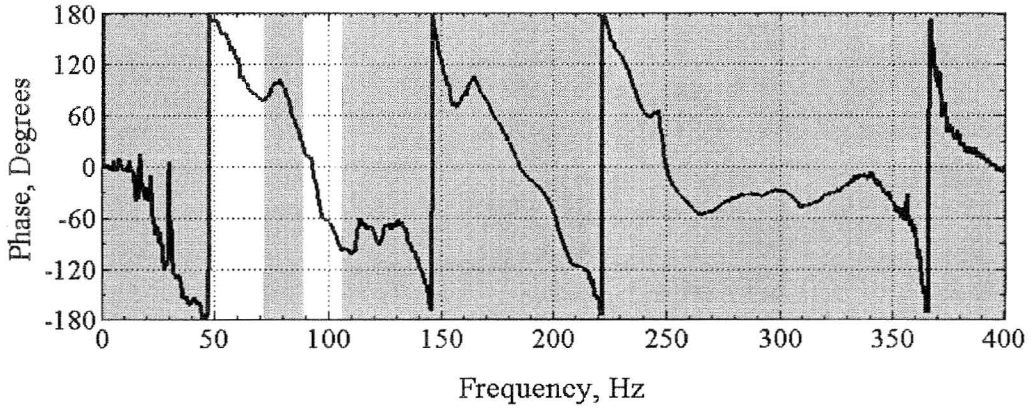

Figure Z.1 Phase Plots Measured by SASW Testing with 6-ft Receiver Spacing (4H6_F_21.DAT)

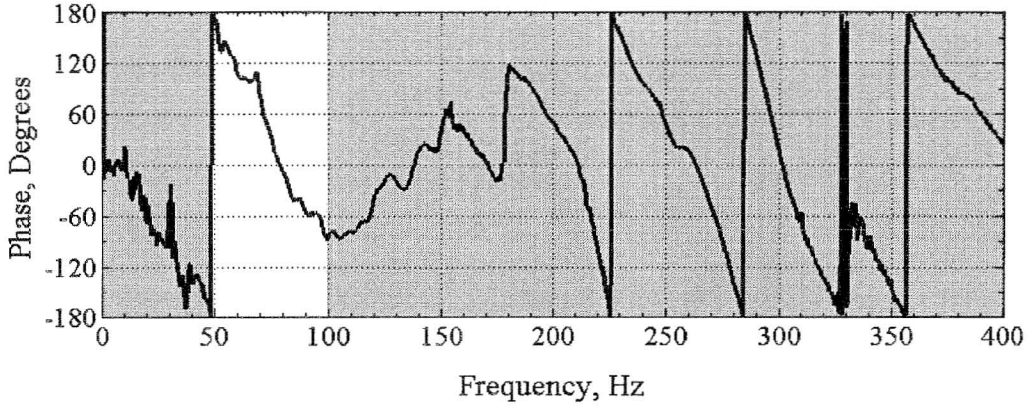

Figure Z.2 Phase Plots Measured by SASW Testing with 6-ft Receiver Spacing (4H7_F_21.DAT)

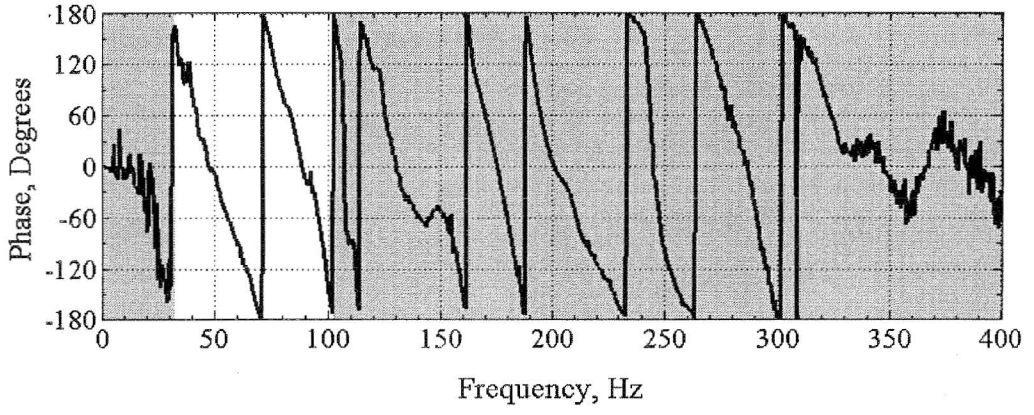

Figure Z.3 Phase Plots Measured by SASW Testing with 12-ft Receiver Spacing (4H6_F_43.DAT)

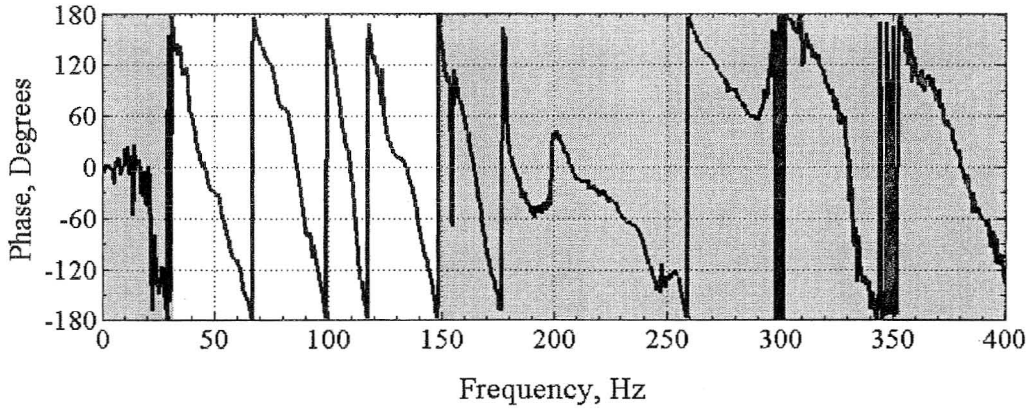

Figure Z.4 Phase Plots Measured by SASW Testing with 12-ft Receiver Spacing (4H7_F_43.DAT)

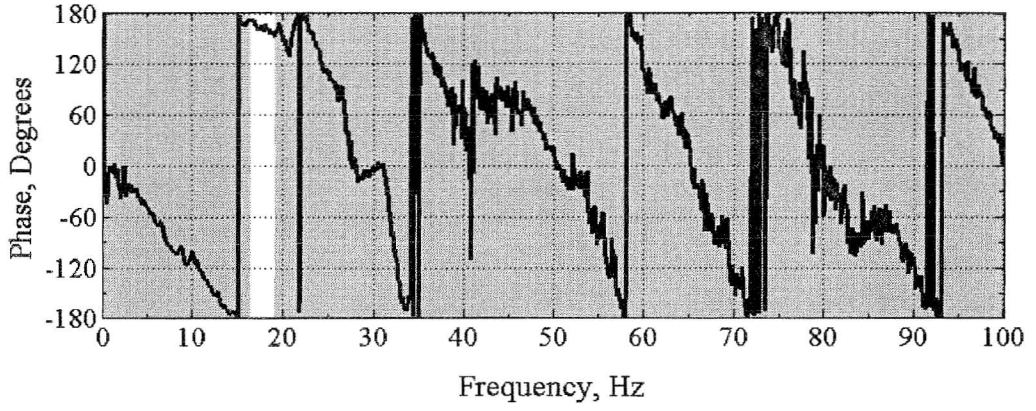

Figure Z.5 Phase Plots Measured by SASW Testing with 25-ft Receiver Spacing (4H1_F_21.DAT)

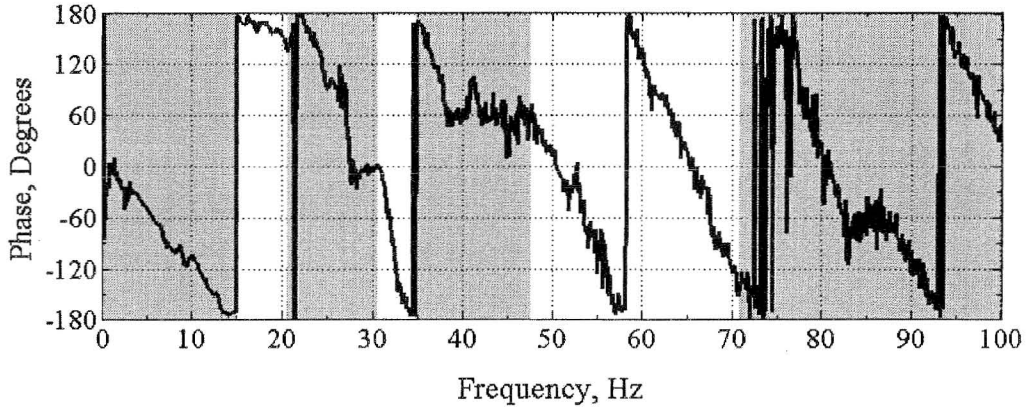

Figure Z.6 Phase Plots Measured by SASW Testing with 25-ft Receiver Spacing (4H2_F_21.DAT)

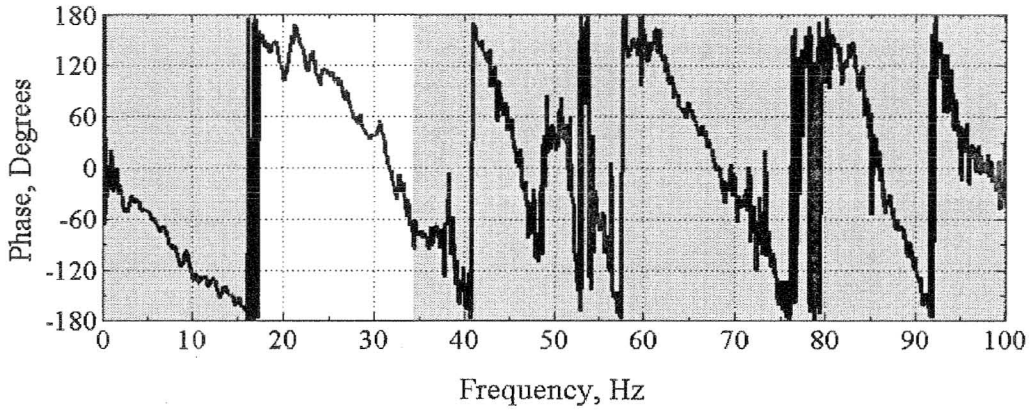

Figure Z.7 Phase Plots Measured by SASW Testing with 25-ft Receiver Spacing (4H2_F_43.DAT)

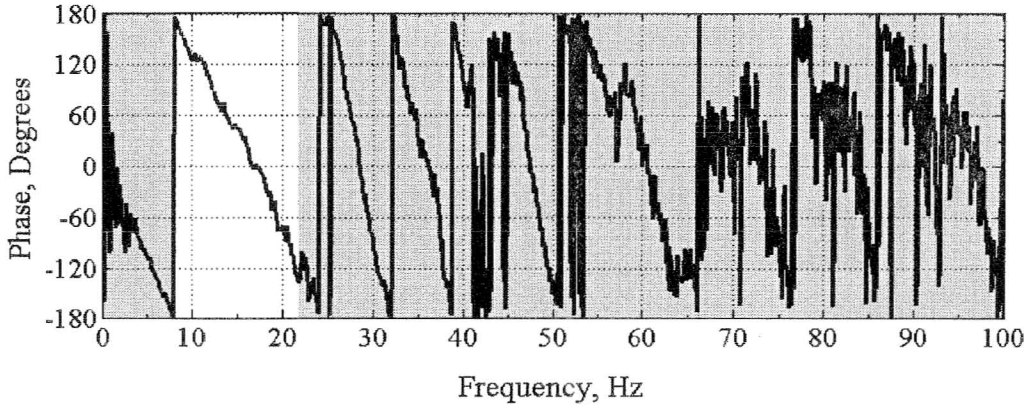

Figure Z.8 Phase Plots Measured by SASW Testing with 50-ft Receiver Spacing (4H1_F_43.DAT)

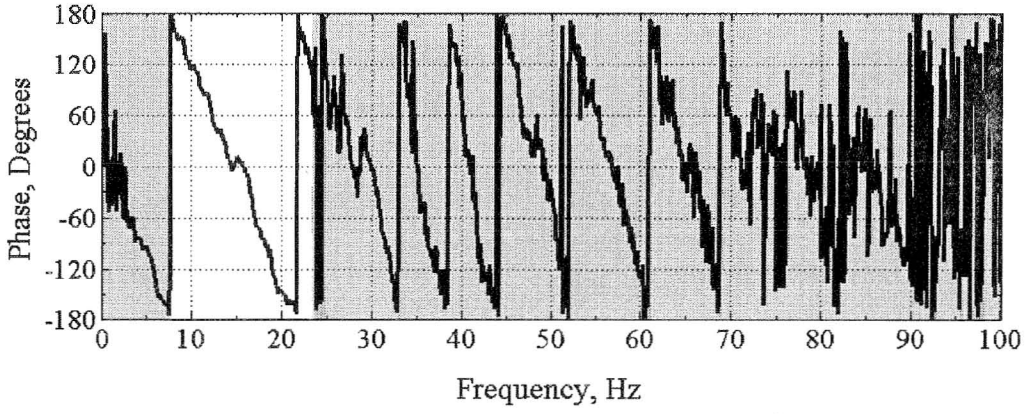

Figure Z.9 Phase Plots Measured by SASW Testing with 50-ft Receiver Spacing (4H3_F_21.DAT)

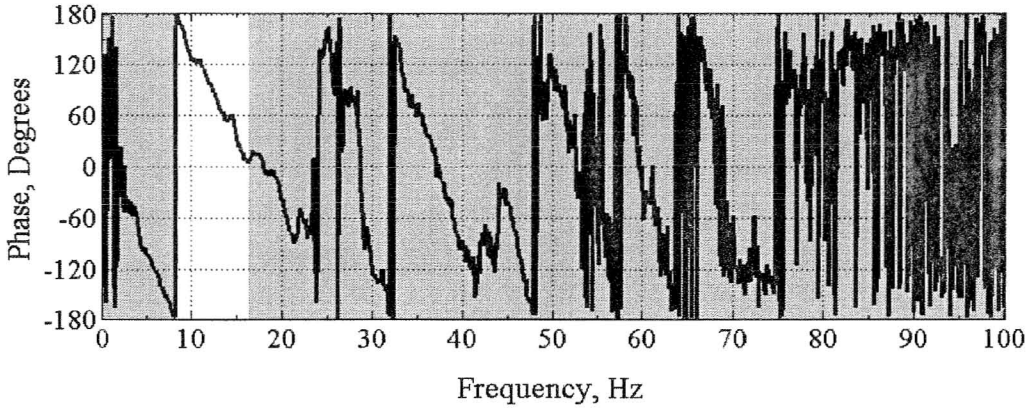

Figure Z.10 Phase Plots Measured by SASW Testing with 50-ft Receiver Spacing (4H3_F_43.DAT)

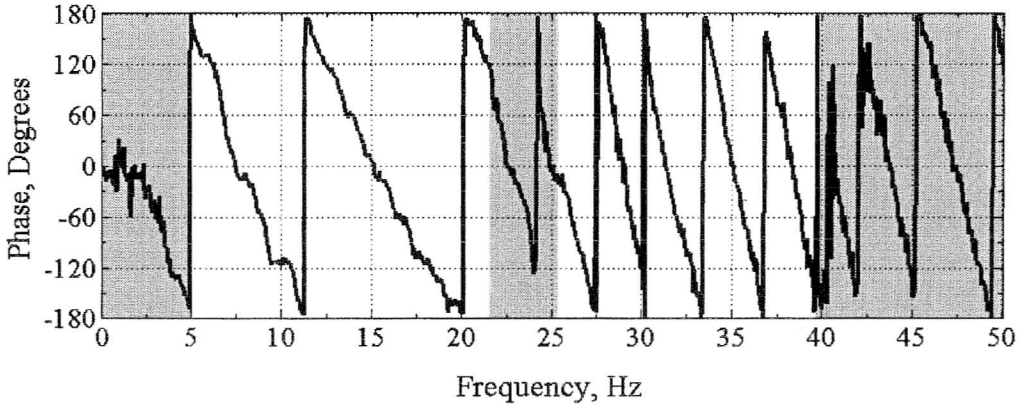

Figure Z.11 Phase Plots Measured by SASW Testing with 100-ft Receiver Spacing (4H4_F_21.DAT)

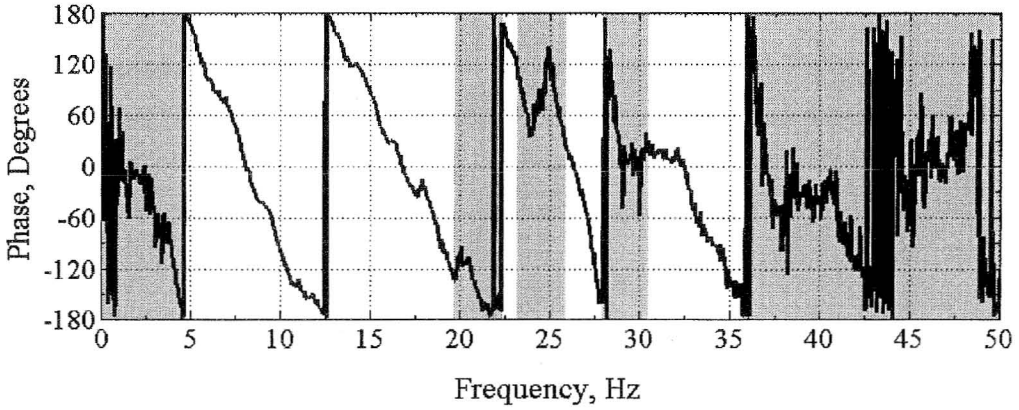

Figure Z.12 Phase Plots Measured by SASW Testing with 100-ft Receiver Spacing (4H4_F_43.DAT)

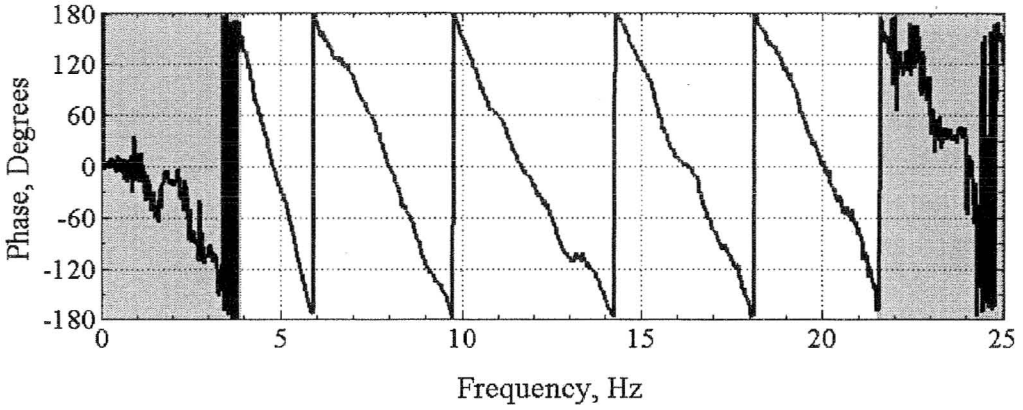

Figure Z.13 Phase Plots Measured by SASW Testing with 200-ft Receiver Spacing (4H5_F_21.DAT)

Table Z.1 Tables of Masking Parameters Used on Data Collected during Fourth Site Visit at Site H

Receiver Spacing (ft)	Masking Interval	Masking Start Frequency, Hz	Masking Stop Frequency, Hz	Number of Jumps	Filename
6	1	0	48	1	4H6_F_21.DAT
	2	71.5	89.5	1	
	3	106	400	-	
6	1	0	49	1	4H7_F_21.DAT
	2	99.5	400	-	
12	1	0	32.5	1	4H6_F_43.DAT
	2	102	400	-	
12	1	0	32	1	4H7_F_43.DAT
	2	148	400	-	
25	1	0	16.38	1	4H1_F_21.DAT
	2	19.12	100	-	
25	1	0	15.12	1	4H2_F_21.DAT
	2	20.62	30.5	1	
	3	34.62	47.62	2	
	4	70.62	100	-	
25	1	0	16.88	1	4H2_F_43.DAT
	2	34.25	100	-	
50	1	0	8.12	1	4H1_F_43.DAT
	2	21.75	100	-	
50	1	0	7.75	1	4H3_F_21.DAT
	2	23.38	100	-	
50	1	0	8.38	1	4H3_F_43.DAT
	2	16.25	100	-	
100	1	0	5	1	4H4_F_21.DAT
	2	21.5	25.31	3	
	3	39.5	50	-	
100	1	0	4.75	1	4H4_F_43.DAT
	2	19.69	22.31	3	
	3	23.13	25.88	3	
	4	27.88	30.5	4	
	5	35.75	50	-	
200	1	0	3.94	1	4H5_F_21.DAT
	2	21.44	25	-	

Performed by Jiabei Yuan Checked by Yin-Cheng Lin

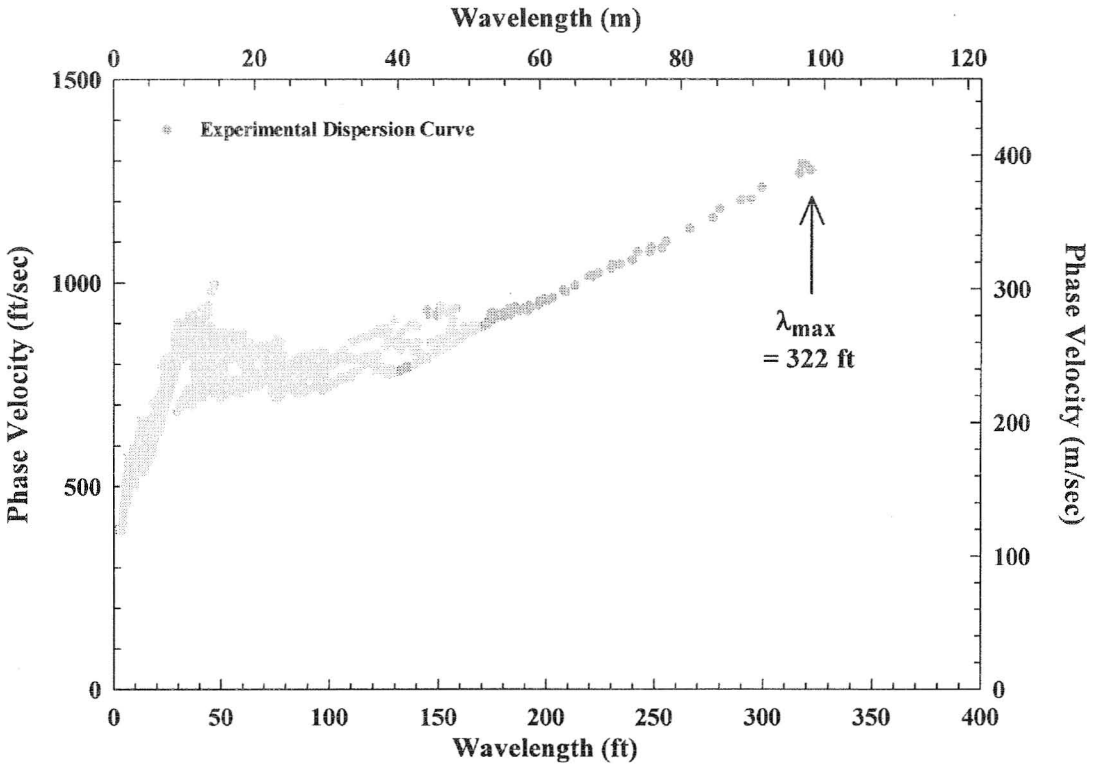

Figure Z.14 Experimental Dispersion Curve Measured during Fourth Site Visit at Site H at Vogtle, GA; Linear Wavelength Axis

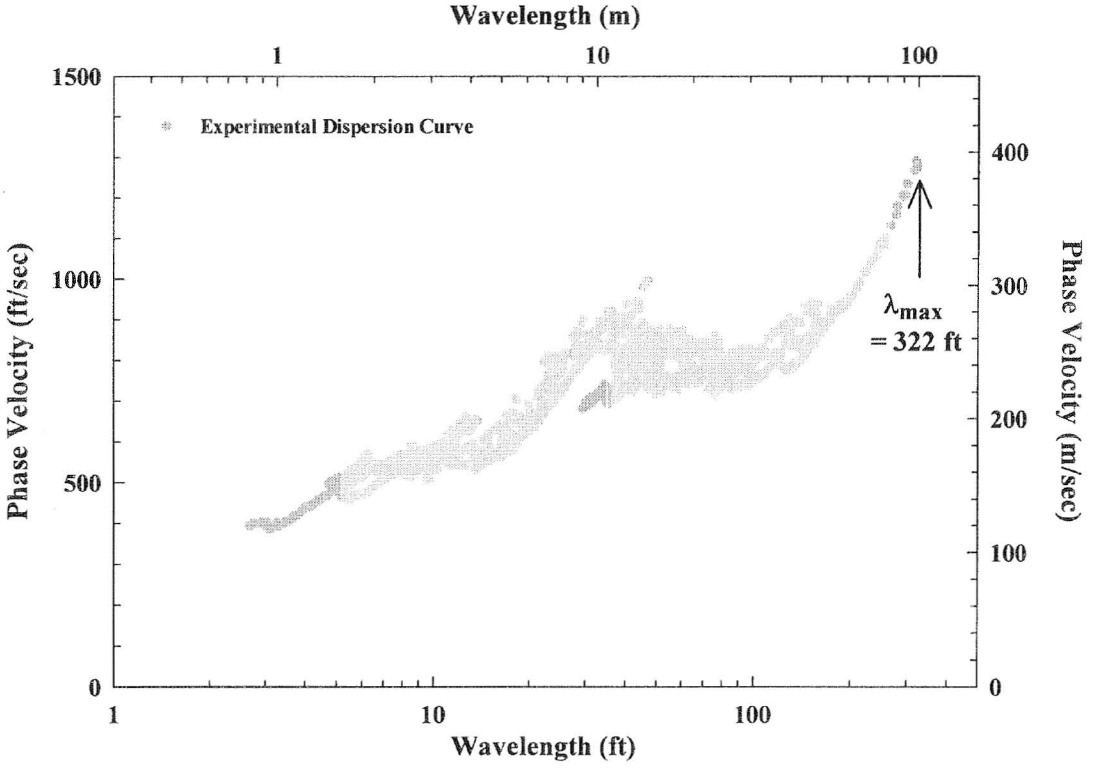

Figure Z.15 Experimental Dispersion Curve Measured during Fourth Site Visit at Site H at Vogtle, GA; Logarithmic Wavelength Axis

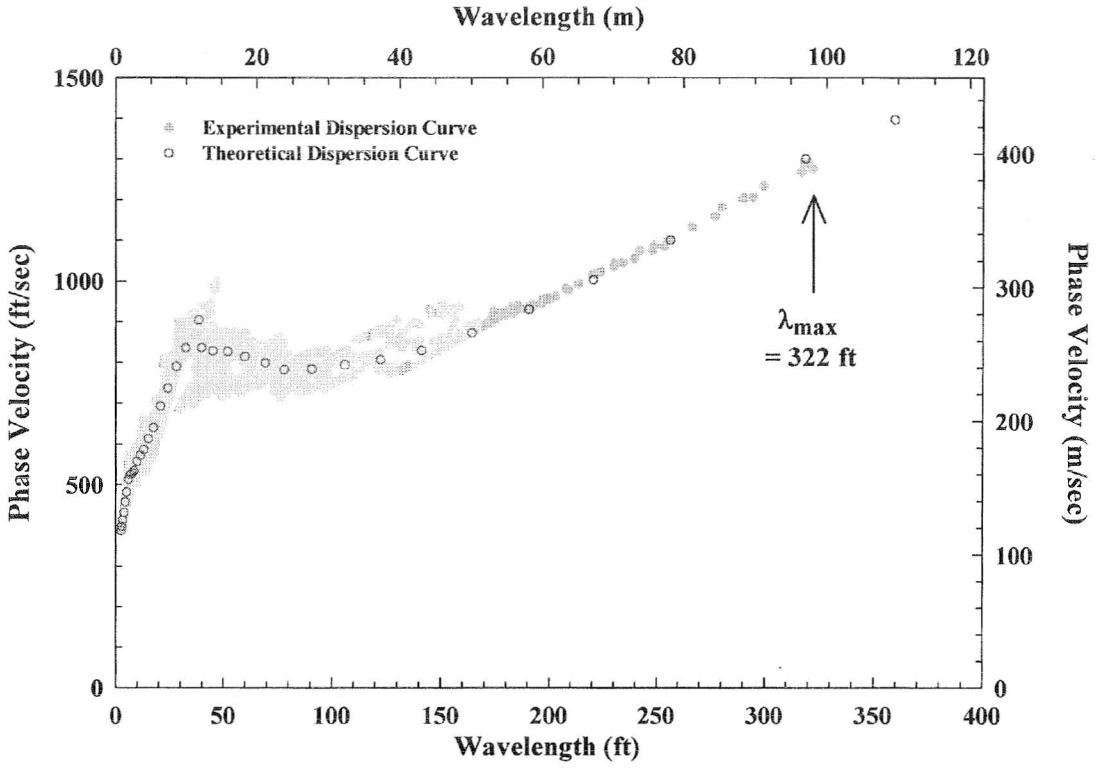

Figure Z.16 Experimental and Theoretical Dispersion Curves from Site H in Fourth Site Visit at Vogtle, GA; Linear Wavelength Axis

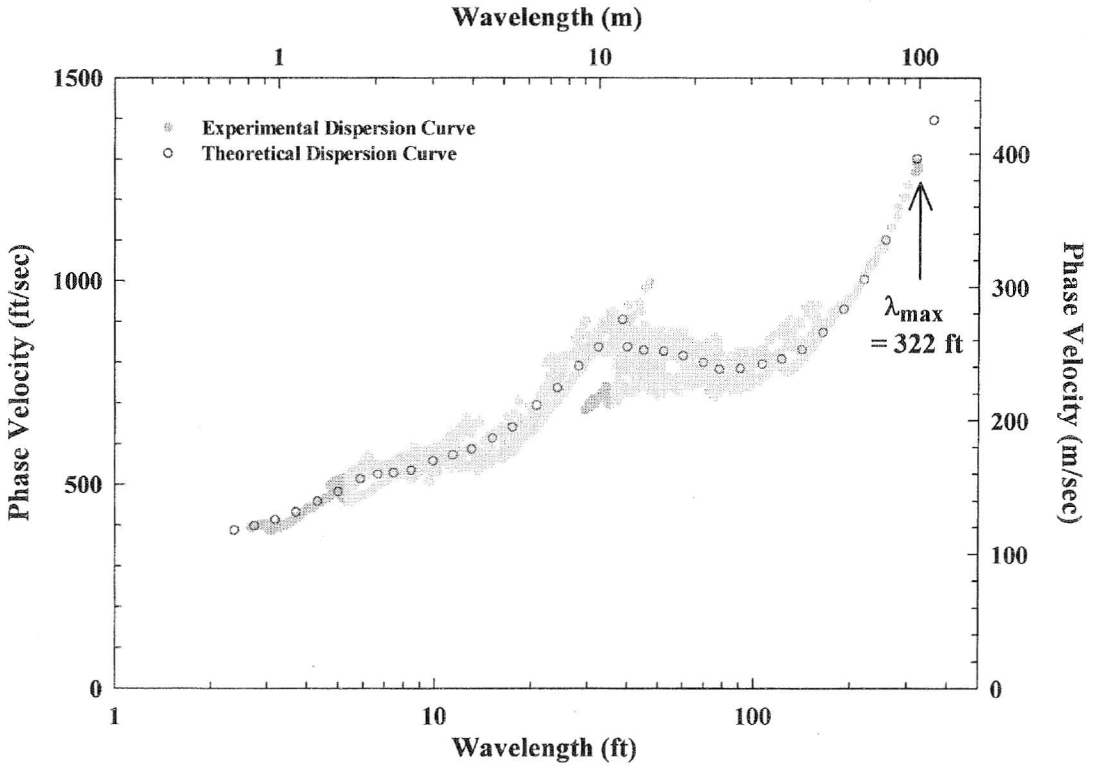

Figure Z.17 Experimental and Theoretical Dispersion Curves from Site H in Fourth Site Visit at Vogtle, GA; Logarithmic Wavelength Axis

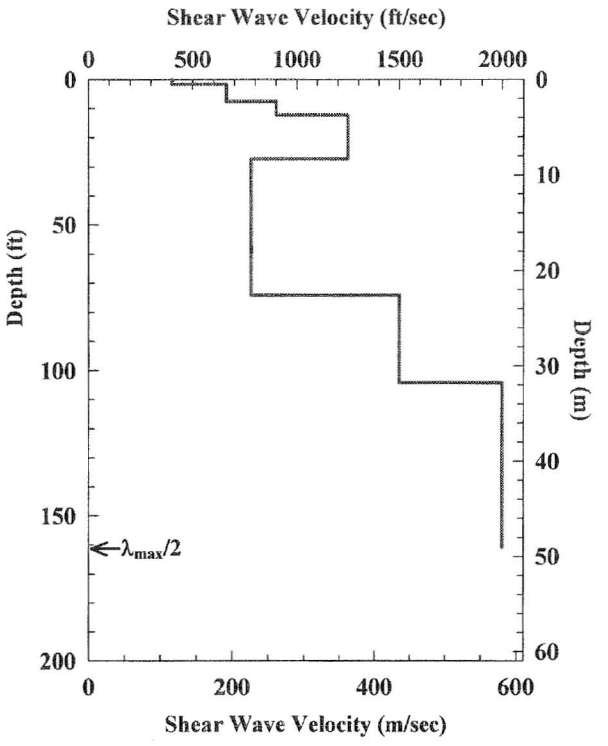

Figure Z.18 Shear Wave Velocity Profile Determined at Site H during Fourth Site Visit at Vogtle, GA

Table Z.2 Profile Parameters Used to Develop Preliminary Theoretical Dispersion Curve at Site H in the Fourth Site Visit at Vogtle, GA

Layer No.	Thickness, ft	Depth to Top of Layer, ft	S-Wave Velocity, ft/s	Assumed Poisson's Ratio	P-Wave Velocity, ft/s	Assumed Total Unit Weight, pcf
1	1.6	0.0	400	0.24	684	125
2	6.0	1.6	660	0.24	1128	125
3	4.6	7.6	900	0.24	1539	125
4	15.0	12.2	1250	0.24	2137	125
5	47.0	27.2	780	0.24	1334	125
6#	30.0	74.2	1500	0.45	5000	135
7#	56.8	104.2	2000	0.40	5000	135
8*#	Half Space	161.0	2000	0.40	5000	135

* Layer below maximum depth of the V_S Profile.
\# Layer below water tatble.

Performed by Yin-Cheng Lin Checked by K. H. Stokoe
Yin-Cheng Lin Kenneth H. Stokoe, II

Appendix AA

Calibration Documents for Geophones and Agilent 35670A Dynamic Signal Analyzer

Calibration Documentation

Calibration Procedure: Mark Products L4 Geophones

Performed: October 19, 2007
Expires: October 19, 2008

1. Equipment Calibrated Using This Procedure:

EQUIPMENT	DESCRIPTION	SERIAL NUMBER
Mark Products L4	Geophones	3770, 3773, 3774,3775

2. NIST Traceable Reference Equipment Used in Calibration:

EQUIPMENT	DESCRIPTION	SERIAL NUMBER	CALIBRATION #	CAL. DATE	EXP. DATE
Agilent 34401A	Digital Multimeter	US36105870	006846	7/16/2007	7/16/2008
Columbia	Accelerometer 3021	2120	998953	8/08/2007	8/08/2008
Columbia	Charge Amplifier 4102M	813	998954	8/08/2007	8/08/2008
Agilent 35670A	Dynamic Signal Analyzer	MY41005676	002104	4/16/2007	4/16/2008

3. Other Previously Verified Equipment Used in Calibration:

EQUIPMENT	DESCRIPTION	SERIAL NUMBER	CAL. DATE	EXP. DATE
Bently-Nevada	19049 Proximitor	120137	10/18/2007	10/18/2008

Performed by : MinJae Jung

Verified by : WonKyoung Choi

Checked by : Kenneth H. Stokoe II

Date : October 19, 2007

Mark Products L-4 Geophone Calibration – 19 October 2007
Calibration Date : 10/19/2007
Expiration Date : 10/19/2008
Performed by Min Jae Jung
(Limited Calibration : Phase Only)

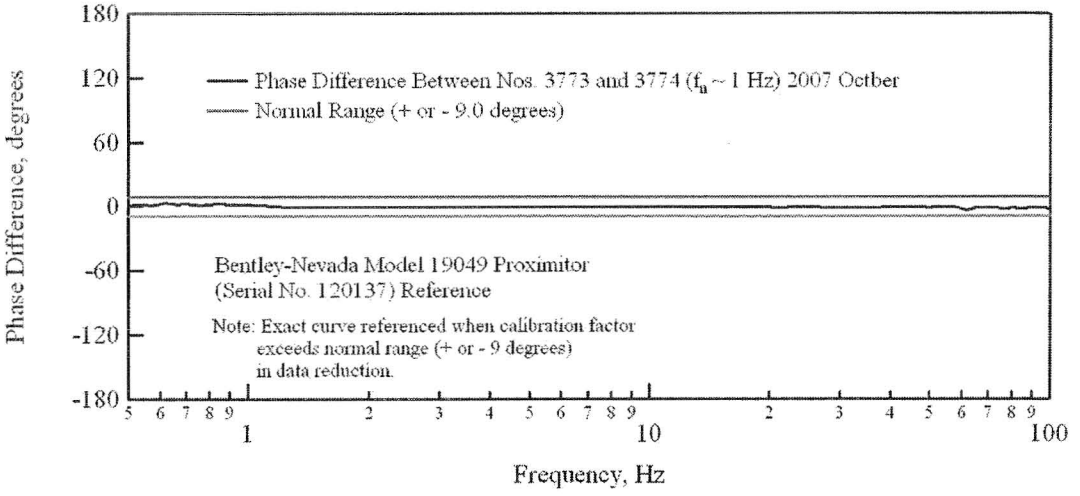

Figure AA1 Phase Difference Between Mark Products L4 Geophones 3773 and 3774, 1- Hz Resonant Frequency; Calibrated Relative to Bently-Nevada Model 19049 Proximitor (Serial No. 120137)- 19 October 2007

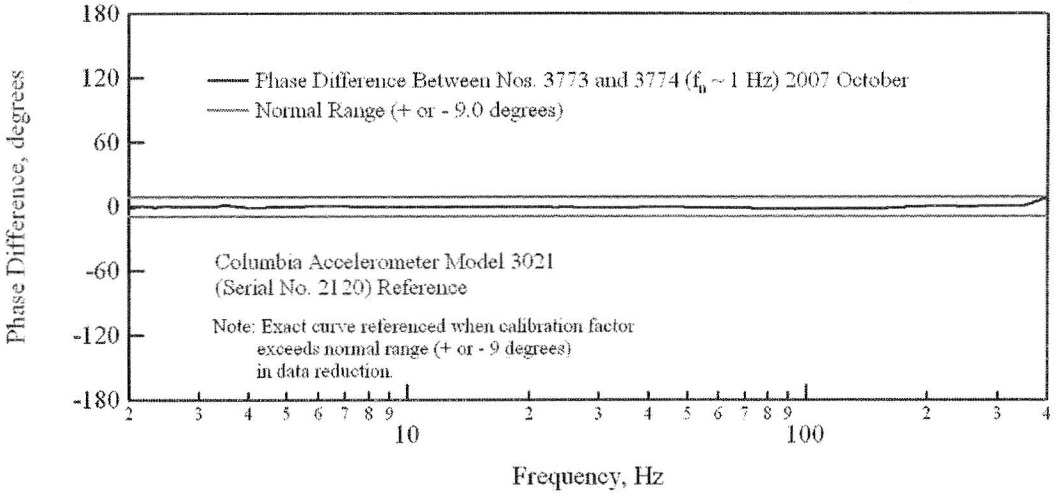

Figure AA2 Phase Difference Between Mark Products L4 Geophones 3773 and 3774, 1- Hz Resonant Frequency; Calibrated Relative to Columbia Accelerometer Model 3021 (Serial No. 2120)- 19 October 2007

Mark Products L-4 Geophone Calibration – 19 October 2007
Calibration Date : 10/19/2007
Expiration Date : 10/19/2008
Performed by Min Jae Jung
(Limited Calibration : Phase Only)

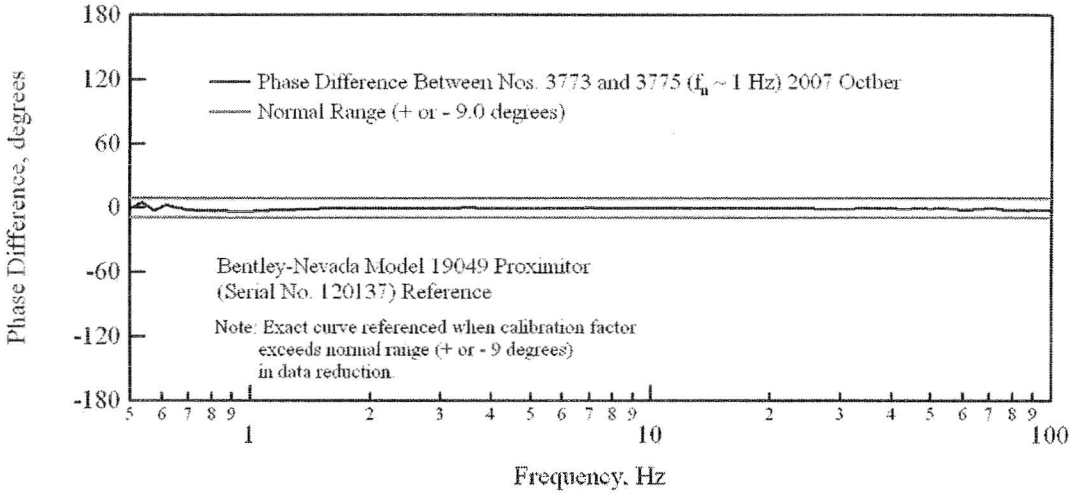

Figure AA3 Phase Difference Between Mark Products L4 Geophones 3773 and 3775, 1- Hz Resonant Frequency; Calibrated Relative to Bently-Nevada Model 19049 Proximitor (Serial No. 120137)- 19 October 2007

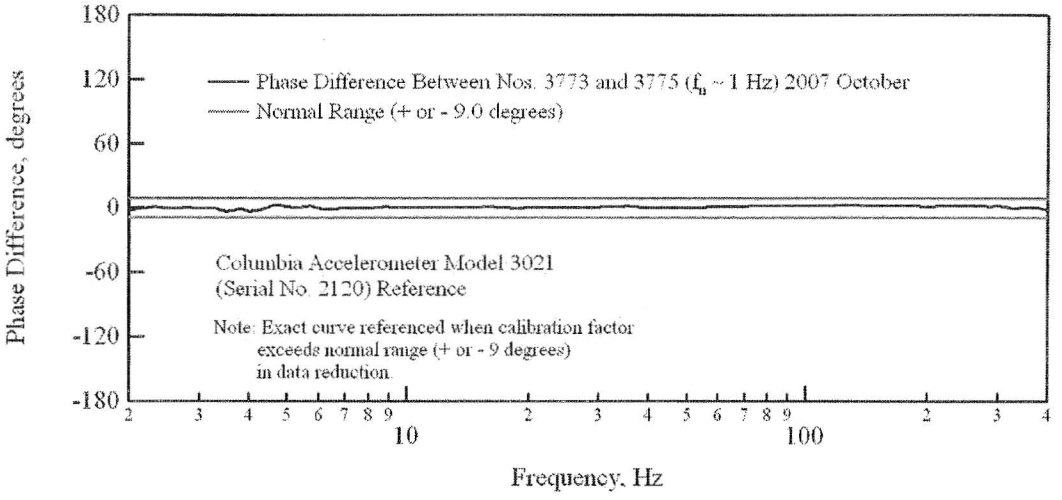

Figure AA4 Phase Difference Between Mark Products L4 Geophones 3773 and 3775, 1- Hz Resonant Frequency; Calibrated Relative to Columbia Accelerometer Model 3021 (Serial No. 2120)- 19 October 2007

Mark Products L-4 Geophone Calibration – 19 October 2007
Calibration Date : 10/19/2007
Expiration Date : 10/19/2008
Performed by Min Jae Jung
(Limited Calibration : Phase Only)

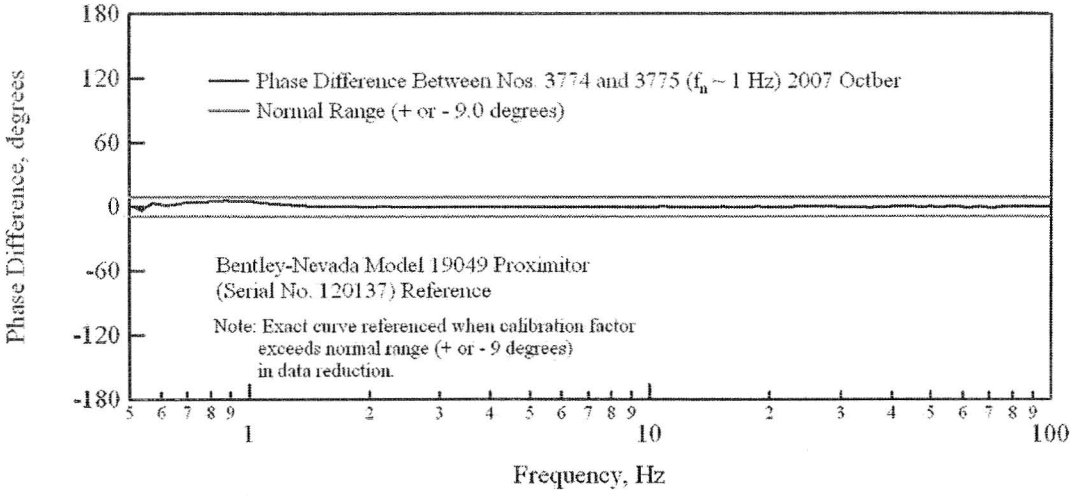

Figure AA5 Phase Difference Between Mark Products L4 Geophones 3774 and 3775, 1- Hz Resonant Frequency; Calibrated Relative to Bently-Nevada Model 19049 Proximitor (Serial No. 120137)- 19 October 2007

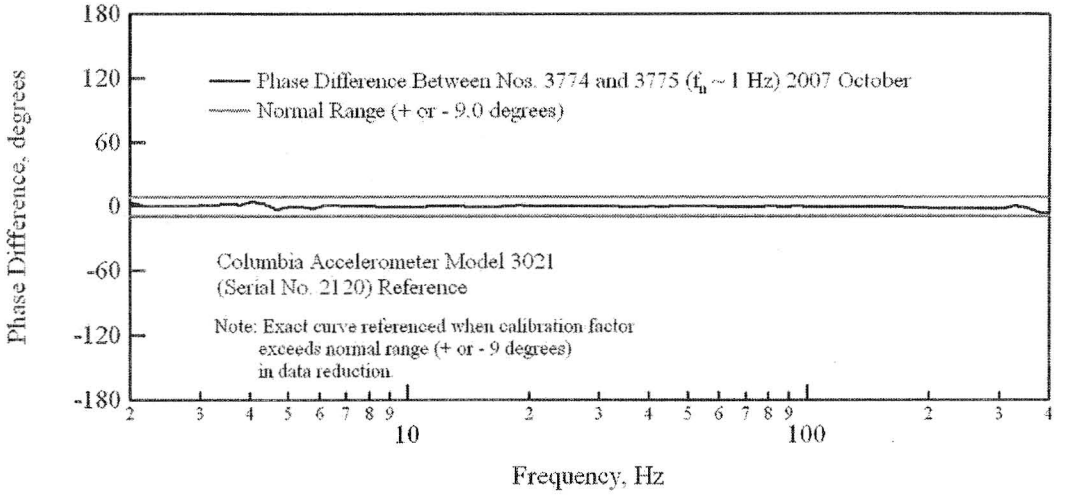

Figure AA6 Phase Difference Between Mark Products L4 Geophones 3774 and 3775, 1- Hz Resonant Frequency; Calibrated Relative to Columbia Accelerometer Model 3021 (Serial No. 2120)- 19 October 2007

Calibration Procedure: Mark Products L10 Geophones

Performed: October 19, 2007
Expires: October 19, 2008

1. Equipment Calibrated Using This Procedure:

EQUIPMENT	DESCRIPTION	SERIAL NUMBER
Mark Products L10	Geophones	92001, 92002, 92003

2. NIST Traceable Reference Equipment Used in Calibration:

EQUIPMENT	DESCRIPTION	SERIAL NUMBER	CALIBRATION #	CAL. DATE	EXP. DATE
Agilent 34401A	Digital Multimeter	US36105870	006846	7/16/2007	7/16/2008
Columbia	Accelerometer 3021	2120	998953	8/08/2007	8/08/2008
Columbia	Charge Amplifier 4102M	813	998954	8/08/2007	8/08/2008
Agilent 35670A	Dynamic Signal Analyzer	MY41005676	002104	4/16/2007	4/16/2008

3. Other Previously Verified Equipment Used in Calibration:

EQUIPMENT	DESCRIPTION	SERIAL NUMBER	CAL. DATE	EXP. DATE
Bently-Nevada	19049 Proximitor	120137	8/14/2006	8/14/2007

Performed by : MinJae Jung

Verified by : WonKyoung Choi

Checked by : Kenneth H. Stokoe II

Date : October 19, 2007

Mark Products L-10 Geophone Calibration – 19 October 2007
Calibration Date : 10/19/2007
Expiration Date : 10/19/2008
Performed by Min Jae Jung
(Limited Calibration : Phase Only)

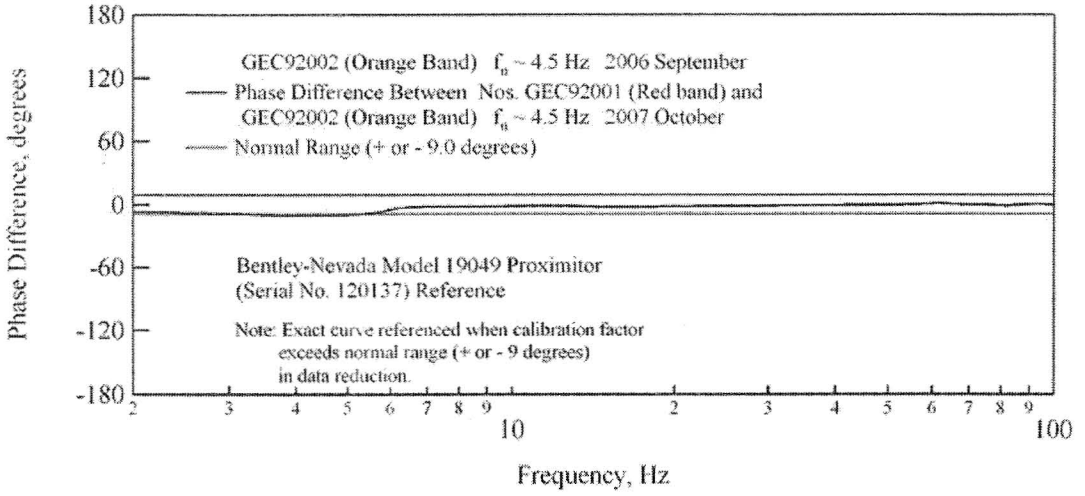

Figure AA7 Phase Difference Between Mark Products L10 Geophones 92001 and 92002, 4.5-Hz Resonant Frequency; Calibrated Relative to Bently-Nevada Model 19049 Proximitor (Serial No. 120137)- 19 October 2007

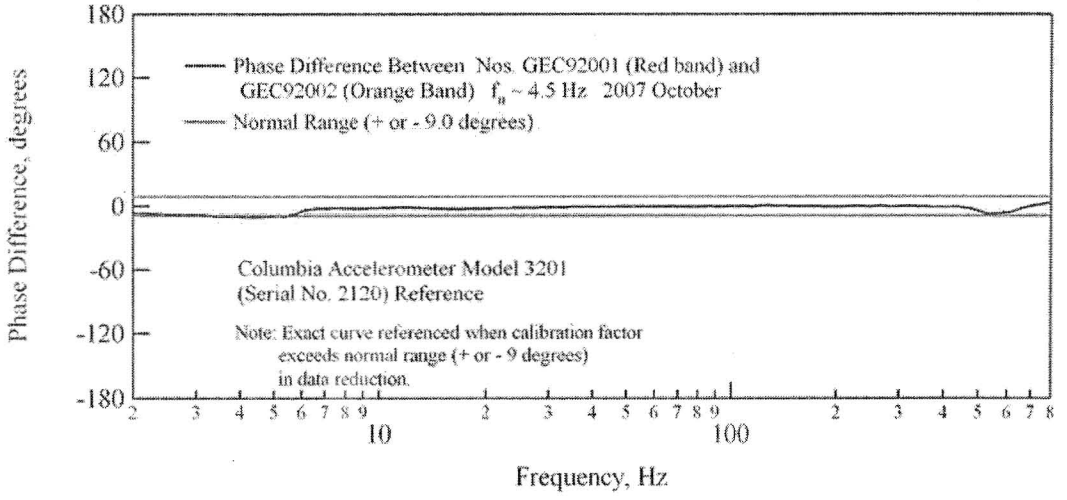

Figure AA8 Phase Difference Between Mark Products L10 Geophones 92001 and 92002, 4.5-Hz Resonant Frequency; Calibrated Relative to Columbia Accelerometer Model 3021 (Serial No. 2120)- 19 October 2007

Mark Products L-10 Geophone Calibration – 19 October 2007
Calibration Date : 10/19/2007
Expiration Date : 10/19/2008
Performed by Min Jae Jung
(Limited Calibration : Phase Only)

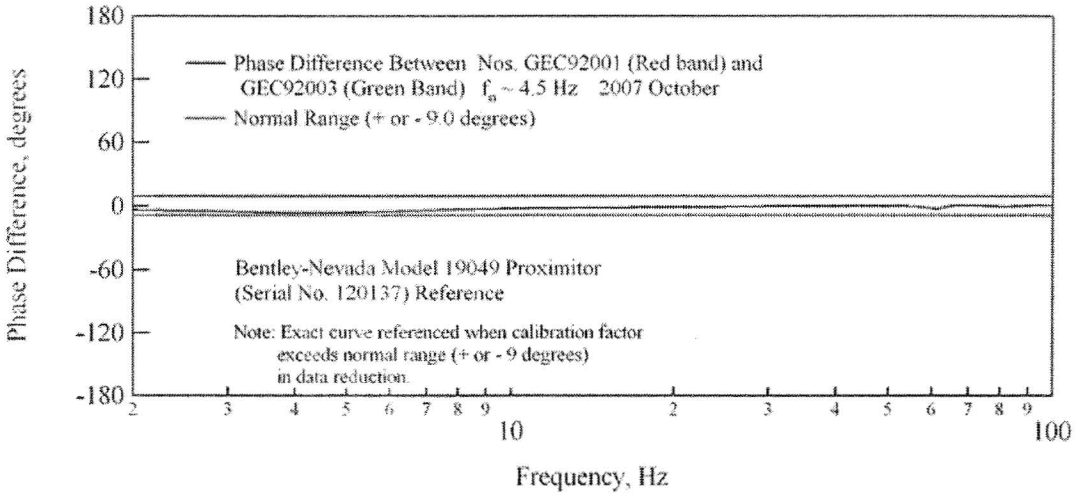

Figure AA9 Phase Difference Between Mark Products L10 Geophones 92001 and 92003, 4.5-Hz Resonant Frequency; Calibrated Relative to Bently-Nevada Model 19049 Proximitor (Serial No. 120137)- 19 October 2007

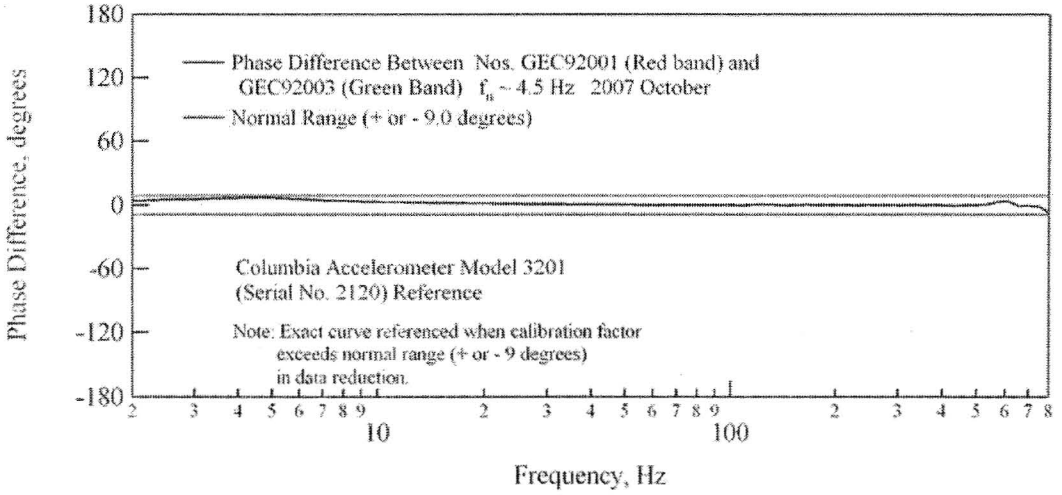

Figure AA10 Phase Difference Between Mark Products L10 Geophones 92001 and 92003, 4.5-Hz Resonant Frequency; Calibrated Relative to Columbia Accelerometer Model 3021 (Serial No. 2120)- 19 October 2007

Mark Products L-10 Geophone Calibration – 19 October 2007
Calibration Date : 10/19/2007
Expiration Date : 10/19/2008
Performed by Min Jae Jung
(Limited Calibration : Phase Only)

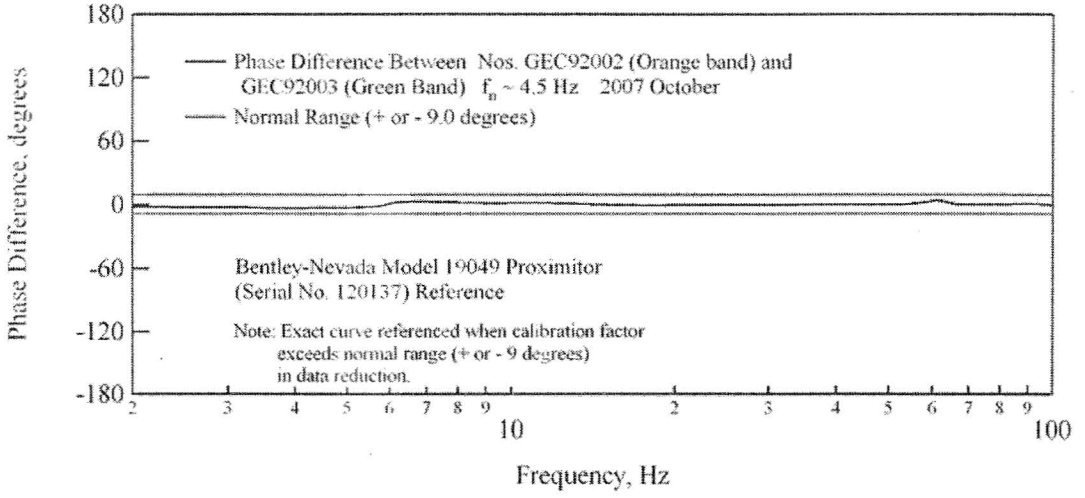

Figure AA11 Phase Difference Between Mark Products L10 Geophones 92002 and 92003, 4.5-Hz Resonant Frequency; Calibrated Relative to Bently-Nevada Model 19049 Proximitor (Serial No. 120137)- 19 October 2007

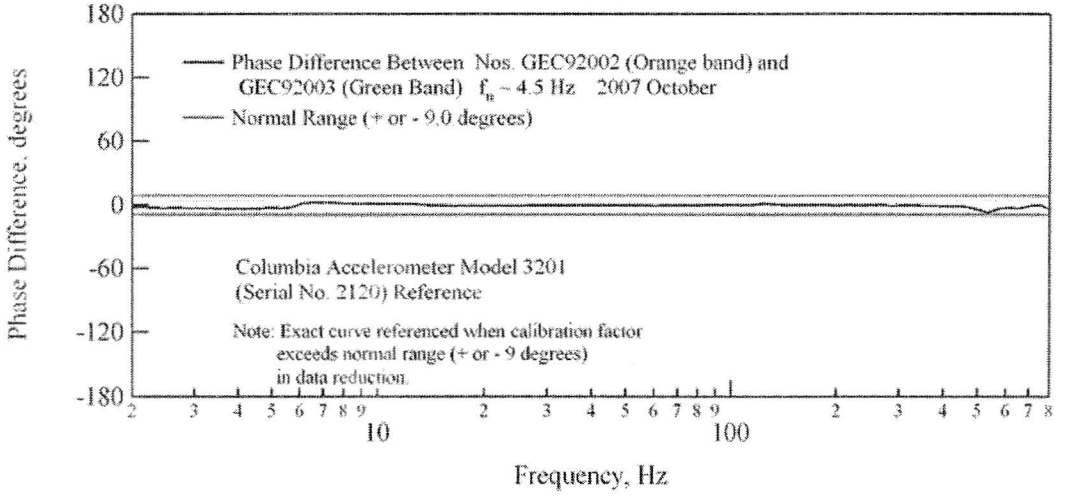

Figure AA12 Phase Difference Between Mark Products L10 Geophones 92002 and 92003, 4.5-Hz Resonant Frequency; Calibrated Relative to Columbia Accelerometer Model 3021 (Serial No. 2120)- 19 October 2007

Calibration Procedure: Geo Space GS-11D Geophones

Performed: December 07, 2007
Expires: December 07, 2008

1. Equipment Calibrated Using This Procedure:

EQUIPMENT	DESCRIPTION	SERIAL NUMBER
Geo Space GS-11D	Geophones	UT07-4.5Hz-02 UT07-4.5Hz-03 UT07-4.5Hz-04

2. NIST Traceable Reference Equipment Used in Calibration:

EQUIPMENT	DESCRIPTION	SERIAL NUMBER	CALIBRATION #	CAL. DATE	EXP. DATE
Agilent 34401A	Digital Multimeter	US36105870	006846	7/16/2007	7/16/2008
Columbia	Accelerometer 3021	2120	998953	8/08/2007	8/08/2008
Columbia	Charge Amplifier 4102M	813	998954	8/08/2007	8/08/2008
Agilent 35670A	Dynamic Signal Analyzer	MY41005676	002104	4/16/2007	4/16/2008

3. Other Previously Verified Equipment Used in Calibration:

EQUIPMENT	DESCRIPTION	SERIAL NUMBER	CAL. DATE	EXP. DATE
Bently-Nevada	19049 Proximitor	120137	10/18/2007	10/18/2008

Performed by : Jiabei Yuan

Verified by : MinJae Jung

Checked by : Kenneth H. Stokoe II

Date : December 07, 2007

GeoSpace GS-11D Geophone Calibration – 07 December 2007
Calibration Date : 12/07/2007
Expiration Date : 12/07/2008
Performed by : Jiabei Yuan
(Limited Calibration : Phase Only)

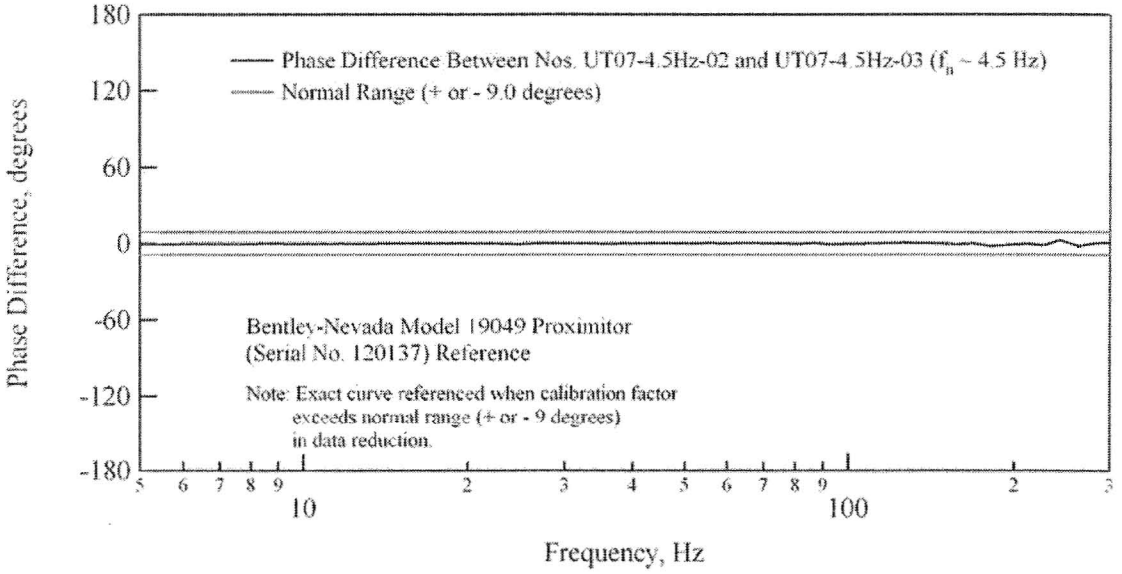

Figure AA13 Phase Difference Between GeoSpace GS-11D Geophones UT07-4.5Hz-02 and UT07-4.5Hz-03, 4.5 - Hz Resonant Frequency; Calibrated Relative to Bently-Nevada Model 19049 Proximitor (Serial No. 120137) - 07 December 2007

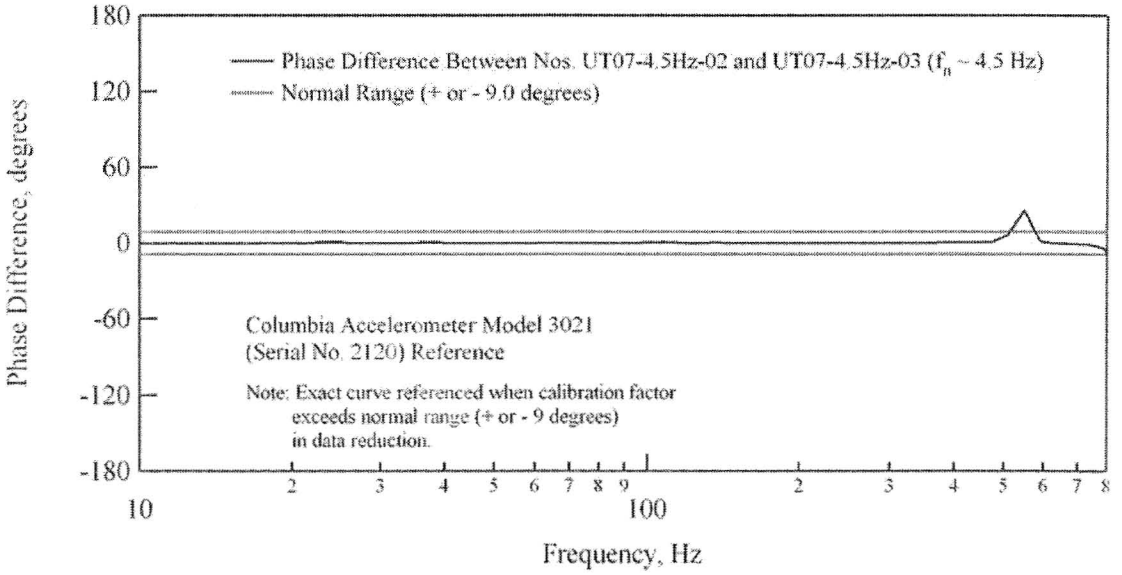

Figure AA14 Phase Difference Between GeoSpace GS-11D Geophones UT07-4.5Hz-02 and UT07-4.5Hz-03, 4.5 - Hz Resonant Frequency; Calibrated Relative to Columbia Accelerometer Model 3021 (Serial No. 2120) - 07 December 2007

GeoSpace GS-11D Geophone Calibration – 07 December 2007
Calibration Date : 12/07/2007
Expiration Date : 12/07/2008
Performed by : Jiabei Yuan
(Limited Calibration : Phase Only)

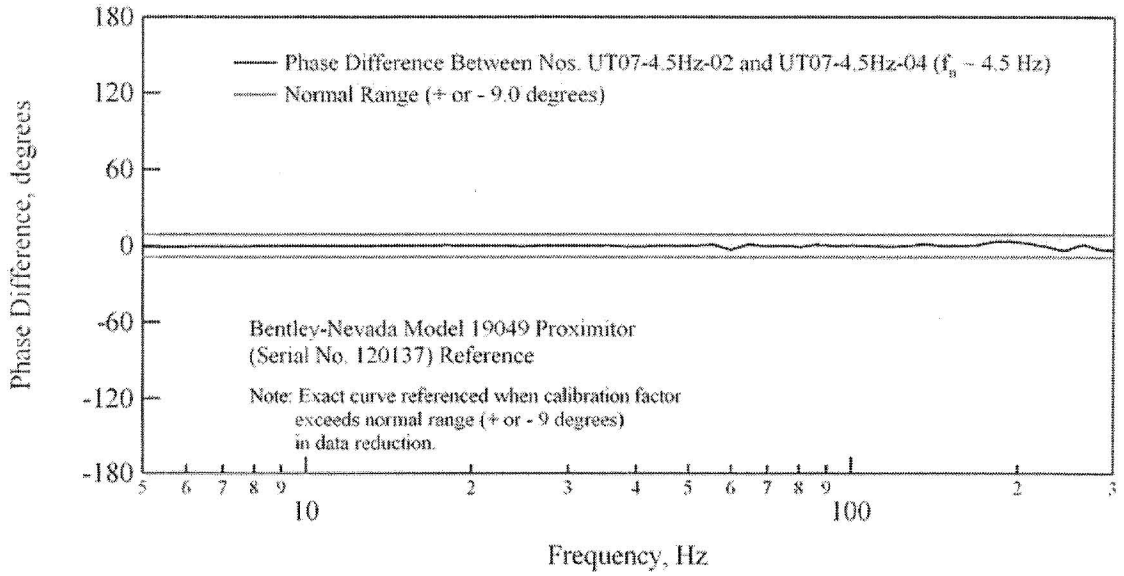

Figure AA15 Phase Difference Between GeoSpace GS-11D Geophones UT07-4.5Hz-02 and UT07-4.5Hz-04, 4.5 - Hz Resonant Frequency; Calibrated Relative to Bently-Nevada Model 19049 Proximitor (Serial No. 120137) - 07 December 2007

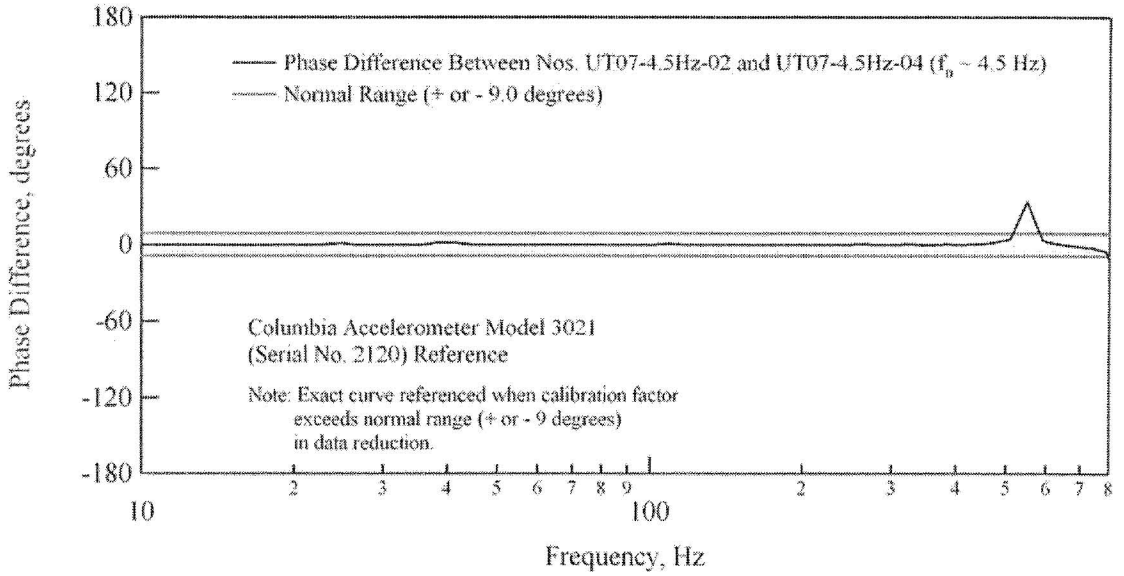

Figure AA16 Phase Difference Between GeoSpace GS-11D Geophones UT07-4.5Hz-02 and UT07-4.5Hz-04, 4.5 - Hz Resonant Frequency; Calibrated Relative to Columbia Accelerometer Model 3021 (Serial No. 2120) - 07 December 2007

GeoSpace GS-11D Geophone Calibration – 07 December 2007
Calibration Date : 12/07/2007
Expiration Date : 12/07/2008
Performed by : Jiabei Yuan
(Limited Calibration : Phase Only)

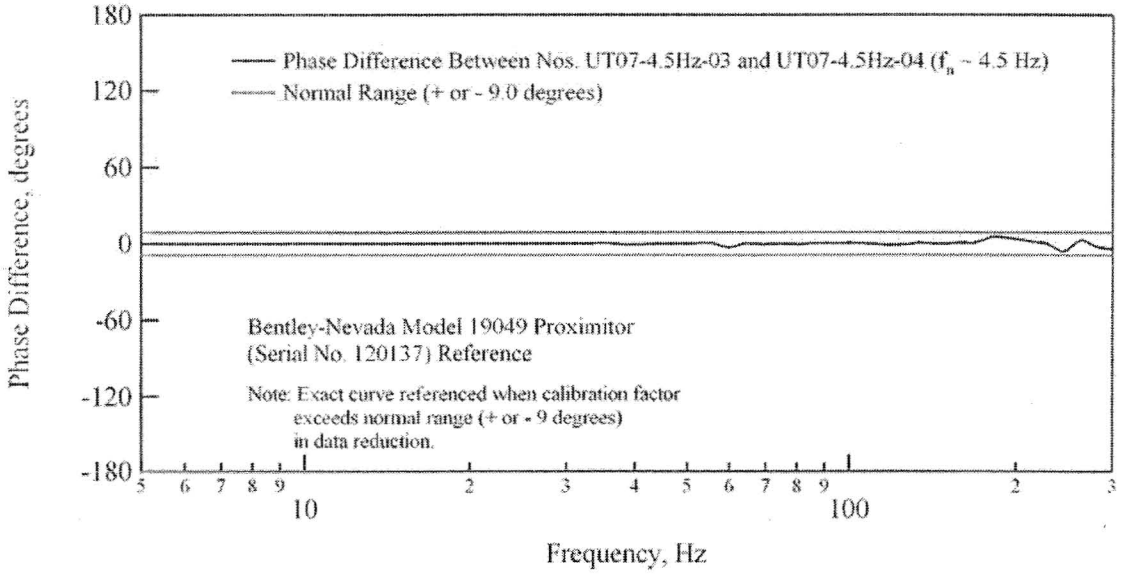

Figure AA17 Phase Difference Between GeoSpace GS-11D Geophones UT07-4.5Hz-03 and UT07-4.5Hz-04, 4.5 - Hz Resonant Frequency; Calibrated Relative to Bently-Nevada Model 19049 Proximitor (Serial No. 120137) - 07 December 2007

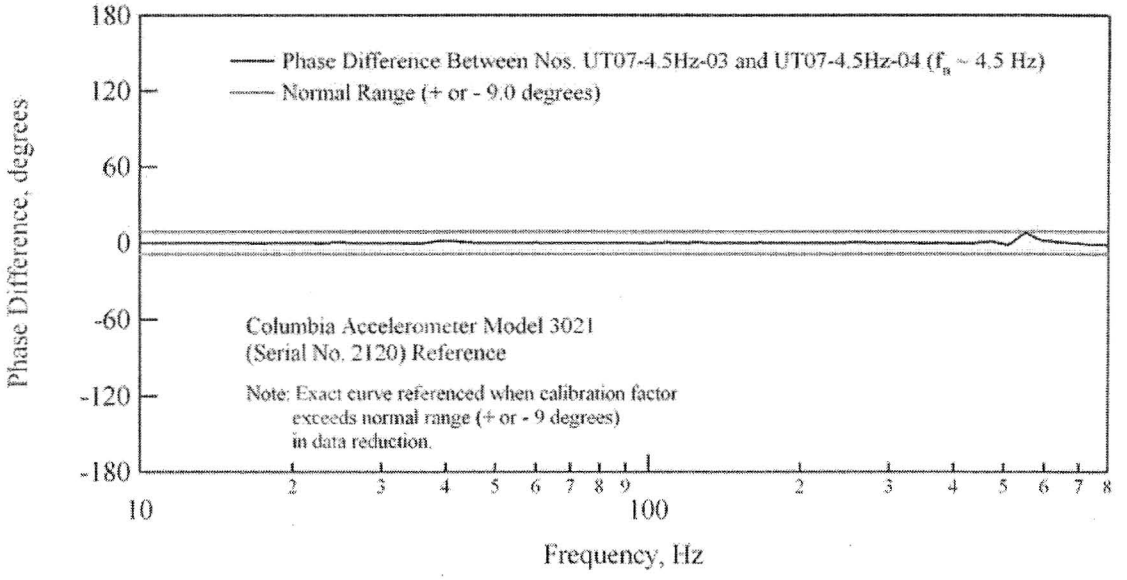

Figure AA18 Phase Difference Between GeoSpace GS-11D Geophones UT07-4.5Hz-03 and UT07-4.5Hz-04, 4.5 - Hz Resonant Frequency; Calibrated Relative to Columbia Accelerometer Model 3021 (Serial No. 2120) - 07 December 2007

Dynamic Signal Analyzer Calibration Documentation (Frequency Domain)
- (Agilent, Serial No. MY41005676)

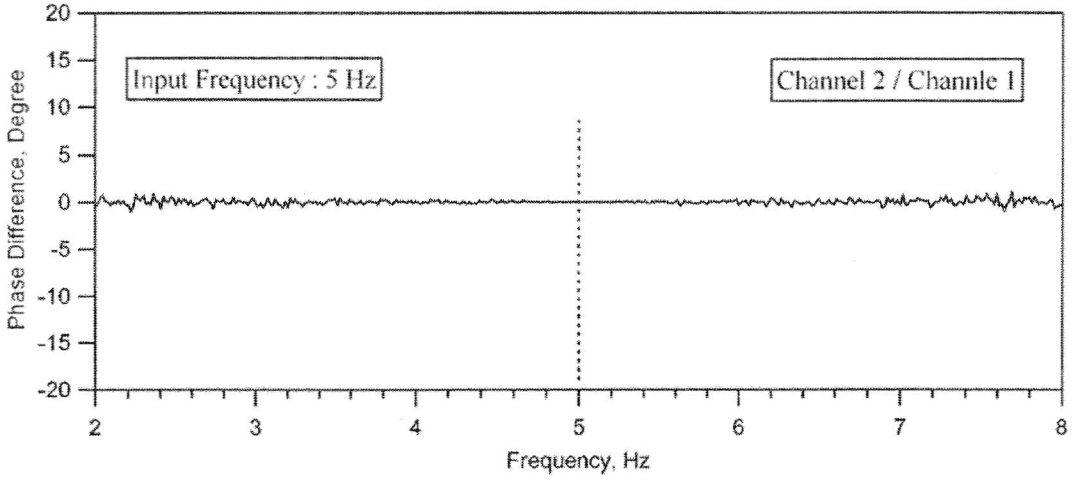

(a)

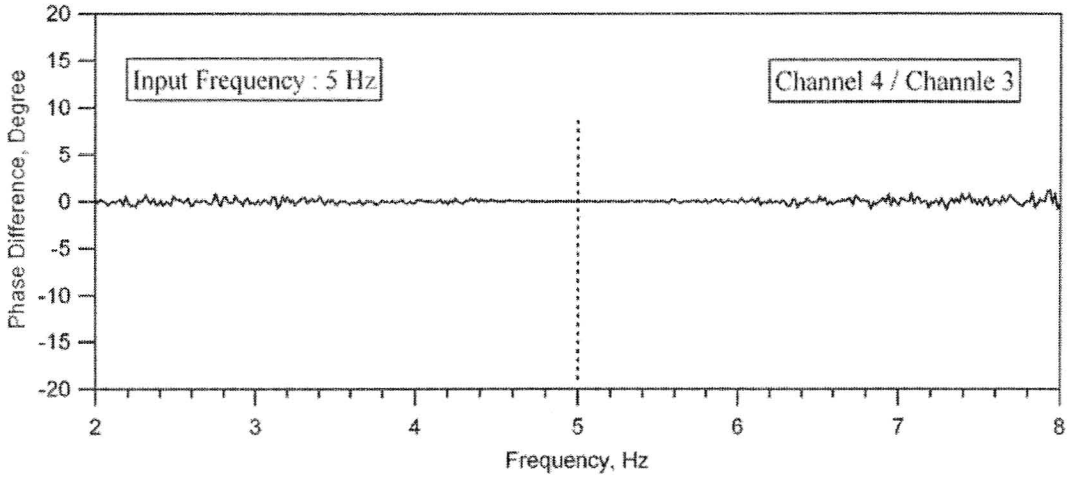

(b)

Figure AA19 Frequency Domain Calibration Records for the Agilent 4-Channel Dynamic Signal Analyzer; (a) Phase Difference Between Channel 2 and Channel 1, (b) Phase Difference Between Channel 4 and Channel 3; 5 Hz Sine Wave Input; December 10, 2007

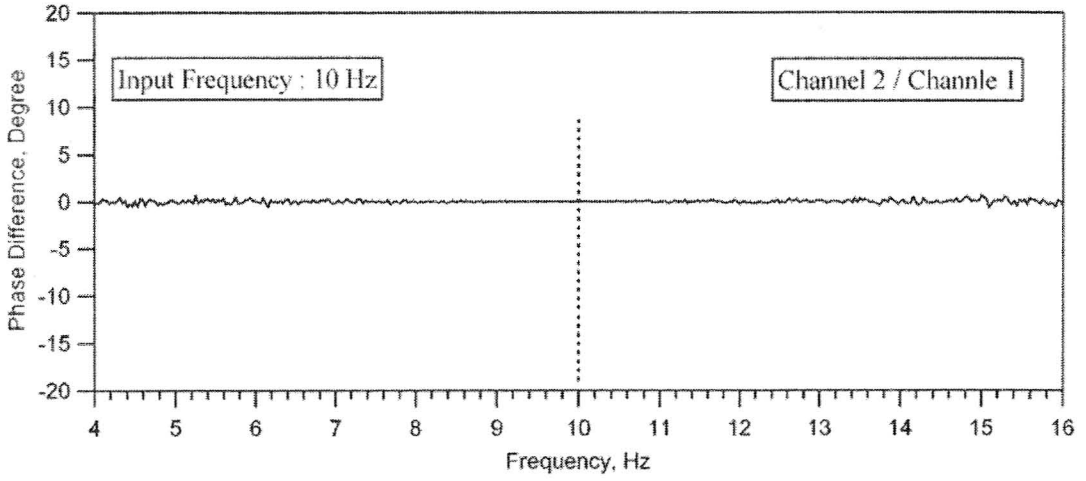

(a)

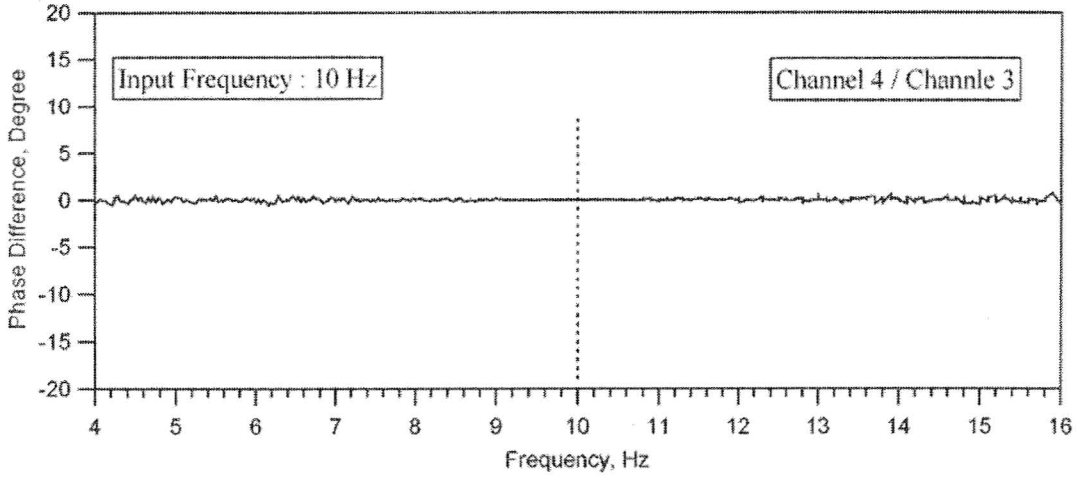

(b)

Figure AA20 Frequency Domain Calibration Records for the Agilent 4-Channel Dynamic Signal Analyzer; (a) Phase Difference Between Channel 2 and Channel 1, (b) Phase Difference Between Channel 4 and Channel 3; 10 Hz Sine Wave Input; December 10, 2007

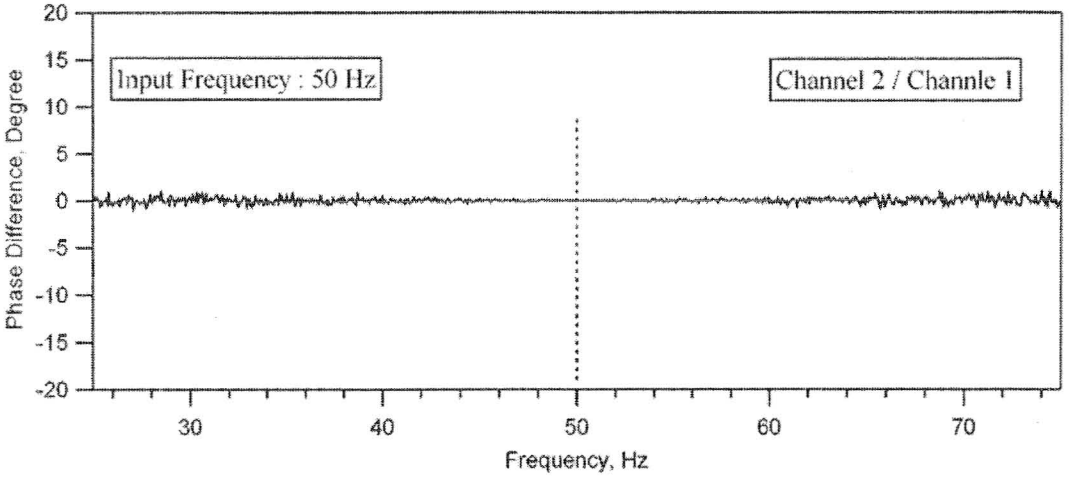

(a)

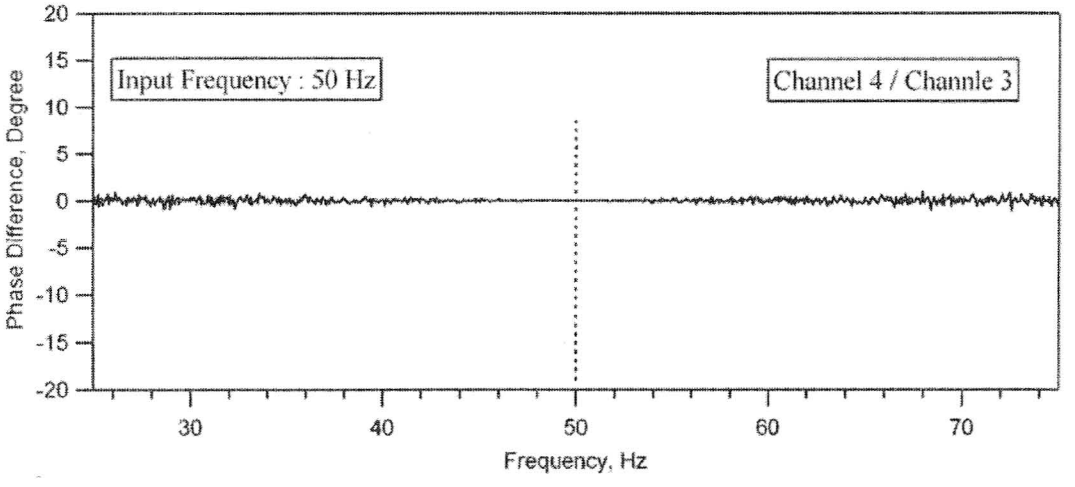

(b)

Figure AA21 Frequency Domain Calibration Records for the Agilent 4-Channel Dynamic Signal Analyzer; (a) Phase Difference Between Channel 2 and Channel 1, (b) Phase Difference Between Channel 4 and Channel 3; 50 Hz Sine Wave Input; December 10, 2007

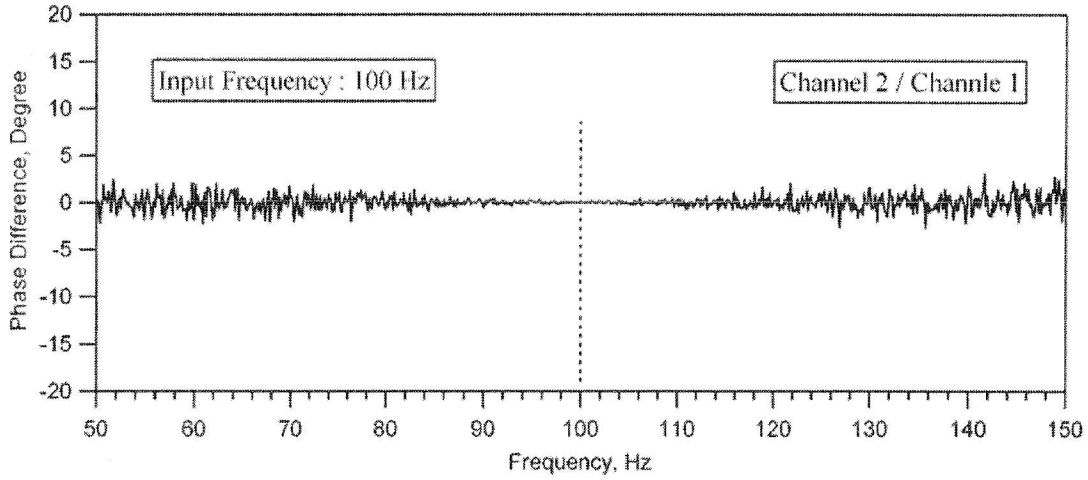

(a)

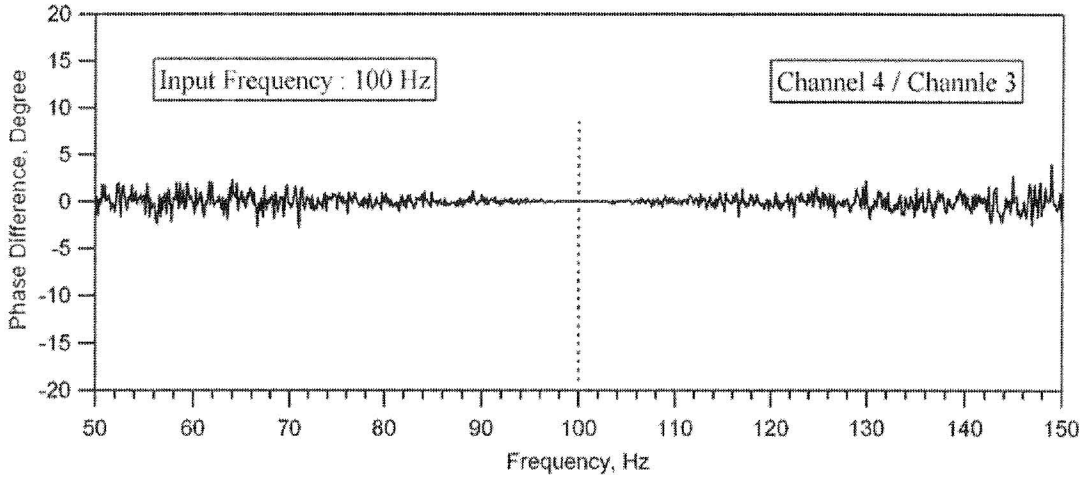

(b)

Figure AA22 Frequency Domain Calibration Records for the Agilent 4-Channel Dynamic Signal Analyzer; (a) Phase Difference Between Channel 2 and Channel 1, (b) Phase Difference Between Channel 4 and Channel 3; 100 Hz Sine Wave Input; December 10, 2007

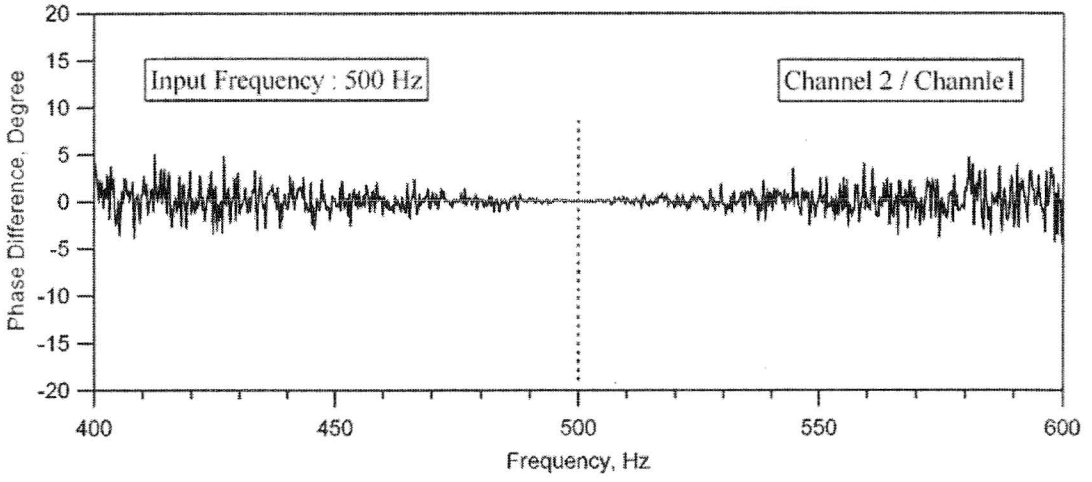

(a)

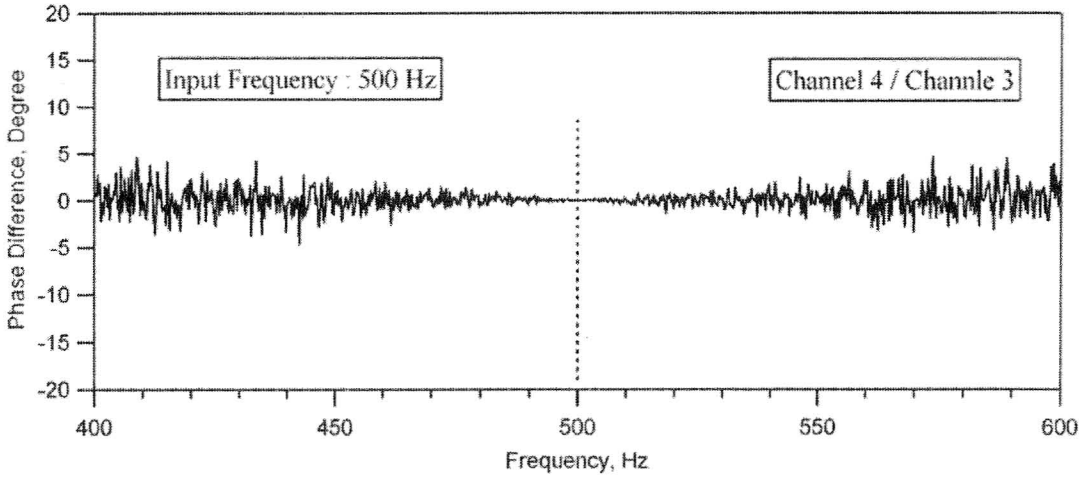

(b)

Figure AA23 Frequency Domain Calibration Records for the Agilent 4-Channel Dynamic Signal Analyzer; (a) Phase Difference Between Channel 2 and Channel 1, (b) Phase Difference Between Channel 4 and Channel 3; 500 Hz Sine Wave Input; December 10, 2007

Table AA1 Calibration Results of Frequency Domain (Agilent Dynamic Signal Analyzer) Performed December 10, 2007

Instrument		4 Channel Dynamic Signal Analyzer		
		Agilent, Serial No.: MY41005676		
Equipement Used		Wavetek Function Generator		
		Model FG2A, Serial No. 912022		
		NIST Traceable Calibration through 5/18/2008		
Calibration Date		12/10/2007		
Input		Sine Wave		
Frequency		**5 Hz**		
Channel No.		Input Amplitude	Phase Difference	
			Expected	Measured
		V	Degree	Degree
2	1	3	0.00000	0.00020
4	3	3	0.00000	0.00083
Input		Sine Wave		
Frequency		**10 Hz**		
Channel No.		Input Amplitude	Phase Difference	
			Expected	Measured
		V	Degree	Degree
2	1	3	0.00000	0.00020
4	3	3	0.00000	0.00067
Input		Sine Wave		
Frequency		**50 Hz**		
Channel No.		Input Amplitude	Phase Difference	
			Expected	Measured
		V	Degree	Degree
2	1	3	0.00000	-0.00017
4	3	3	0.00000	-0.00064
Input		Sine Wave		
Frequency		**100 Hz**		
Channel No.		Input Amplitude	Phase Difference	
			Expected	Measured
		V	Degree	Degree
2	1	3	0.00000	0.00049
4	3	3	0.00000	-0.00022
Input		Sine Wave		
Frequency		**500 Hz**		
Channel No.		Input Amplitude	Phase Difference	
			Expected	Measured
		V	Degree	Degree
2	1	3	0.00000	0.00095
4	3	3	0.00000	0.00011

Appendix AB

Verification of Forward Modeling Method Employed in WinSASW

AB.1 INTRODUCTION

WinSASW 1.23 (Ref. AB1) utilizes the dynamic stiffness matrix method, which was presented by Ref. AB2, to generate a theoretical phase velocity dispersion curve of surface waves generated during Spectral-Analysis-of-Surface-Wave (SASW) testing. Implementation of the Kausel-Roesset formulation was verified through comparisons of the theoretical phase velocity dispersion curves found in the scientific literature with the dispersion curves generated with WinSASW 1.23.

For the verification of the WinSASW 1.23 forward modeling routine, one comparison is shown. This comparison uses an earth profile and a corresponding theoretical phase velocity dispersion curve published in the literature (Ref. AB3).

In the following sections, the soil profile and corresponding theoretical phase velocity dispersion curve are presented. These curves are then compared with the one generated for the same profile with WinSASW 1.23.

AB.2 VERIFICATION THROUGH COMPARISONS

AB.2.1 Comparison of WinSASW 1.23 and G.F. Panza (1980)

The soil profile used in this comparison, which is found in "The Solution of the Inverse Problem in Geophysical Interpretation (Ref. AB3)," is shown in Figure AB1. The theoretical phase velocity dispersion curve generated by WinSASW 1.23 and the one from this article are compared in Figure AB2.

In this comparison, an excellent match between the two dispersion curves is observed. It appears that there are small differences in the low-period portion of the plot (10 to 20 seconds). One explanation for this variation is that the dispersion relation from the literature was digitized from the figure presented in the paper. However, this difference is minor and can be disregarded. Also, it should be noted, that the two-dimensional (2-D) model option in WinSASW 1.23 was used in the comparison. This model assumes plane Rayleigh waves and the fundamental mode.

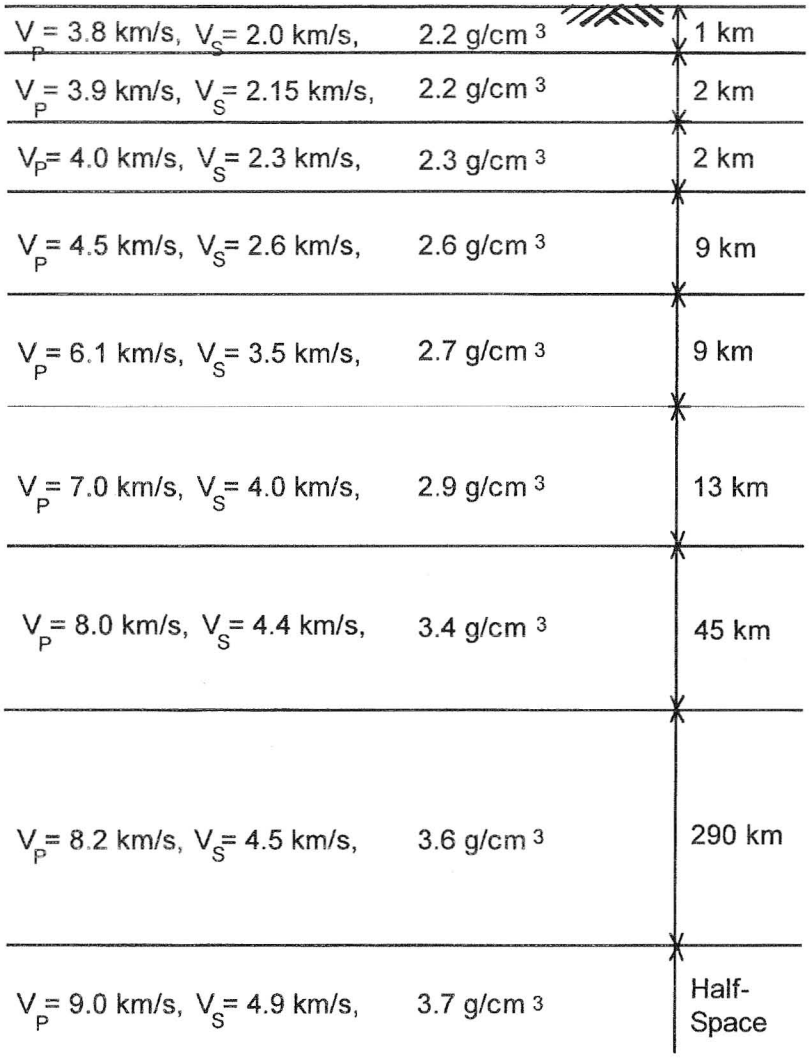

where V_P = P-wave velocity ,
V_S = S-wave velocity, and
ρ = mass density.

Figure AB1 Soil Profile Used in the Calculation of the Theoretical Phase Velocity Dispersion Curves Shown in Figure AB2

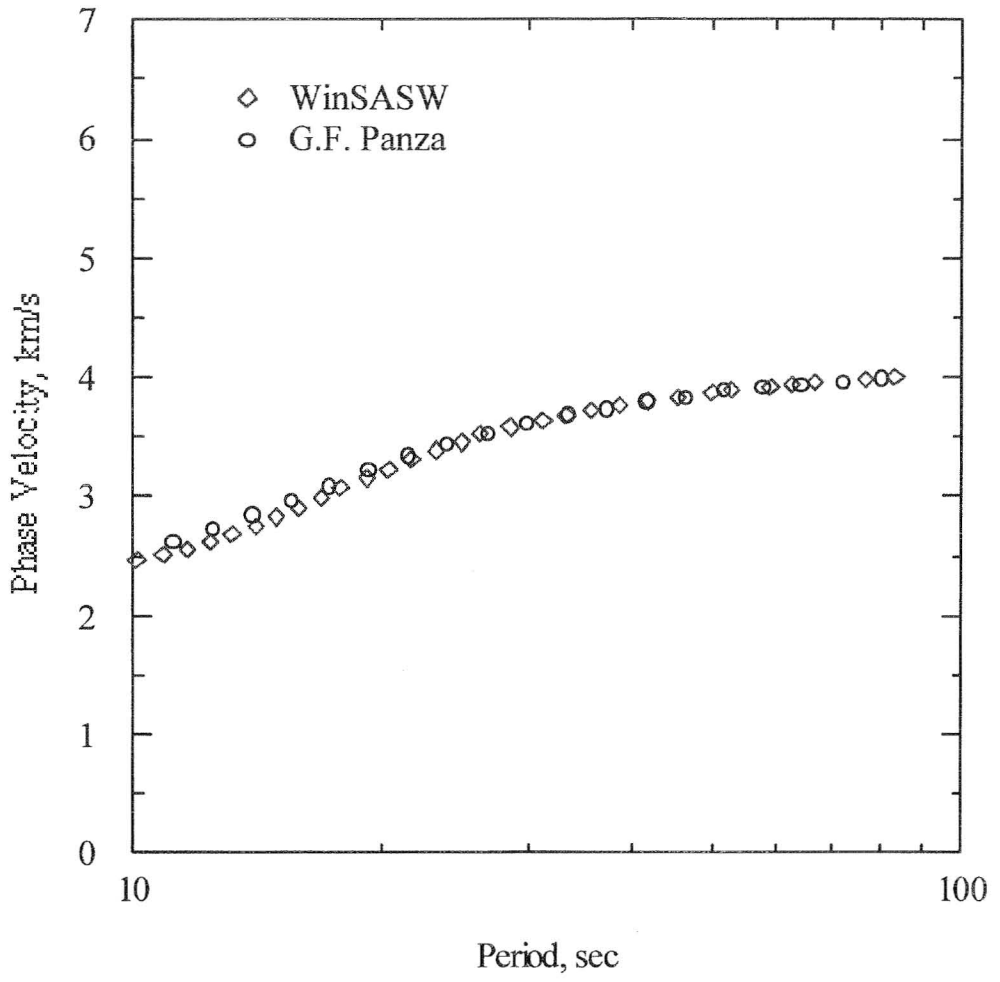

Figure AB2 Comparison of Theoretical Phase Velocity Dispersion Curves from WinSASW 1.23 and from Panza's (1980) Article

AB.2.2 3-Dimensional Solution

The 3-dimensional model option in WinSASW 1.23 is used to analyze the SASW data collected in the field. The differences between the 2-dimensional and 3-dimensional models are not as significant as might be expected. The 2-dimensional solution models a linear wave front in a rectangular coordinate system and only includes Rayleigh-type surface waves, while the 3-dimensional solution models curved wave fronts in an axi-symmetric coordinate system. The 3-dimensional solution also includes effects of body waves. For real sites, the differences between the 2-dimensional and 3-dimensional solutions are generally not very significant. A comparison between the 2-dimensional and the 3-dimensional solutions for the soil profile shown in Figure AB1 is presented in Figure AB3. The only minor difference between these dispersion curves is at wavelengths between 30 km and 110 km that is caused by the effects of body waves

because of the larger velocity contrast between Layer 4 (V_S = 2.6 km/s) and Layer 5 (V_S = 3.5 km/s).

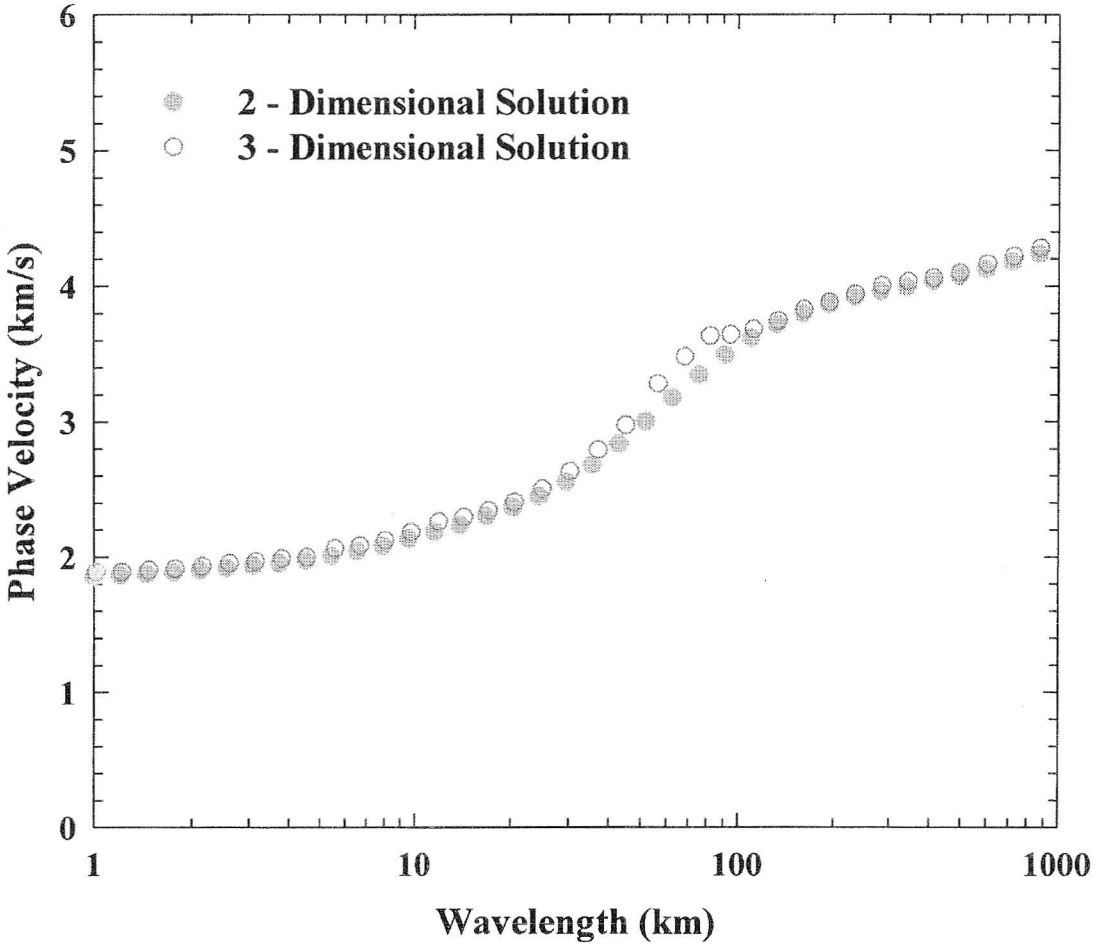

Figure AB3 Comparison Between 2-Dimensional and 3-Dimensional Dispersion Solutions Obtained from WinSASW 1.23 Using the Soil Profile Shown in Figure AB1

AB.3 SUMMARY

Based on the comparison of the WinSASW 1.23 solution with the solution in the literature, as shown in Figure AB2, the forward modeling routine in WinSASW 1.23 is considered to be robust and reliable.

AB.4 REFERENCES

AB1. Joh, S.-H., Stokoe, K.H., II, and Roesset, J.M., 1993, "WinSASW, Data Reduction and Analysis Program for SASW Measurement," Manual of Computer Program WinSASW, the University of Texas at Austin

AB2. Kausel, C. and Roesset, J.M., 1981, "Stiffness Matrices for Layered Soils," Bulletin of the Seismological Society of America, Vol. 71, No. 6

AB3. Panza, G.F., 1980, "The Resolving Power of Seismic Surface Waves with Respect to Crust and Upper Mantle Structural Models," in The Solution of the Inverse Problem in Geophysical Interpretation, R. Cassinis (ed.), Plenum Press, New York, 1981

Appendix AC

Benefits and Limitations of the SASW Method

Benefits and Limitations of the SASW Method

The SASW method has several advantages over conventional seismic field methods in evaluating shear wave velocity profiles. First, the SASW method is both nondestructive and nonintrusive, and can therefore be performed without greatly affecting the surrounding environment. Secondly, because the SASW method does not require a borehole for the test to be performed, it can be conducted rather quickly (about 2 sites to V_S-profile depths around 500 to 800 ft per 10-hour day) and an extensive amount of ground can be investigated. This coverage is a significant advantage over borehole methods which investigate localized areas in and around the borehole. The SASW method can be a useful tool to supplement the information from borehole methods in order to fill in V_S information between boreholes. Thirdly, the SASW method is global in nature, measuring soil and rock properties over large lateral extents approximately equal to the depth of the V_S profile. Fourthly, the SASW method operates using wavelengths that are within the range of wavelengths excited by earthquakes (although they are considerably shorter than the longest wavelength excited by earthquakes). Therefore, for earthquake applications, the SASW method provides soil and rock stiffness as over a range in wavelengths that is appropriate for earthquake analysis.

Although there are several advantages gained from using the SASW method, some limitations exist that should be understood by the user of this information. First, the theoretical model used to determine the shear wave velocity profile at a site is a one-dimensional layered model, meaning there is an assumption of no lateral variation in shear wave velocity and layer thickness across the extent of the receiver array (hence uniform horizontal layers). Therefore, the profile that is presented represents a 1-D layered model that fits the measured dispersion data. It should be noted that lateral variability can be observed qualitatively from mismatches in the individual experimental dispersion curves from adjacent receiver spacings. When these cases occur, they are noted by a footnote attached to the final V_S profile and may also result in multiple interpretations and/or a reduced V_S-profile depth. Secondly, successful implementation of the SASW method requires that multiple receiver spacings are used at one site. This poses some difficultly when creating a single theoretical dispersion curve to match the experimental dispersion curve. Because the actual receiver spacing is not used, the

theoretical dispersion curve is calculated assuming that the receivers are located 2λ and 4λ (λ is wavelength) from the source. Past research has shown that this assumption does not greatly affect the final shear wave velocity profile determined at most sites.

It is important to understand that as the wavelength used in SASW testing increases, and hence the depth of penetration increases, the surface wave propagates through a greater soil volume. The resolution of the SASW method (ability to detect changes in velocity and thickness at depth) decreases as wavelength increases because larger volumes of soil are being sampled as wavelength increases. Therefore, the SASW resolution is best near the surface and decreases at greater depths in the profile. For these analyses, the shear wave velocity profiles are presented to a maximum depth of approximately 0.5 times the longest wavelength recorded in the field. The maximum profile depth is based on the fact that most of the surface wave particle motion is occurring at depths less than 0.5 times the longest wavelength. The step-wise V_S model used in the SASW analysis reflects the general trend in the shear wave velocity profile to this depth (0.5 times the longest wavelength).